Universidade de Aveiro Departamento de Electrónica, Telecomunicações e Informática,
2017

Bruno Ricardo Lito Reis

Desenvolvimento de um laboratório de rádio frequência de baixo custo

Development of a low cost RF Lab

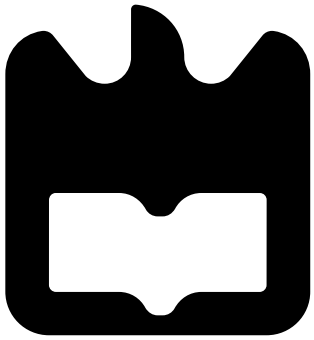

Bruno Ricardo Lito Reis

Development of a low cost RF Lab

Dissertação apresentada à Universidade de Aveiro para cumprimento dos requisitos necessários à obtenção do grau de Mestre em Engenharia Electrónica e Telecomunicações, realizada sob a orientação científica de Pedro Miguel Ribeiro Lavrador e Pedro Miguel da Silva Cabral, Professores do Departamento de Electrónica, Telecomunicações e Informática da Universidade de Aveiro.

Dissertation presented to the University of Aveiro for the fulfillment of the requisites necessary to obtain the degree of Master In Electronics and Telecommunication Engineering, developed under the scientific guidance of Pedro Miguel Ribeiro Lavrador and Pedro Miguel da Silva Cabral, Professors in the Department of Electronics, Telecommunications and Informatics of the University of Aveiro.

o júri / the jury

presidente / president	**Professor Doutor José Carlos Esteves Duarte Pedro** Professor Catedrático da Universidade de Aveiro
vogais / examiners committee	**Professor Doutor Pedro Miguel Ribeiro Lavrador** Professor Auxiliar da Universidade de Aveiro (orientador)
	Doutor Pedro Miguel Duarte Cruz Gestor de Desenvolvimento de Negócio na empresa Controlar Lda (Arguente)

agradecimentos / acknowledgements

Gostaria de agradecer à minha família pelo apoio prestado durante todos estes anos.
Agradeço à Sílvia pelo apoio e pela incansável paciência.

Gostaria também de agradecer aos Professores Pedro Lavrador e Pedro Cabral por toda a ajuda e tempo disponibilizado.
Agradeço ao Filipe Barradas por toda a ajuda prestada durante a realização do trabalho.

Resumo

Com o aumento dos serviços de rede móvel disponíveis é necessária uma utilização mais eficiente dos recursos disponíveis. Para conseguir isso, são necessárias ferramentas de simulação e equipamentos de medida com boa precisão. A comunidade científica tem proposto novos equipamentos que permitem uma melhor caracterização de dispositivos de rádio frequência, como o Vector Network Analyzer (VNA). Neste trabalho são desenvolvidos alguns instrumentos de medida, usando componentes comerciais versáteis e de baixo custo. Os instrumentos implementados são um medidor de potência, um osciloscópio e um VNA. Para o medidor de potência é utilizado um detector de potência e uma Field Programmable Gate Array (FPGA) para processar e exibir o resultado. Para o oscilloscópio e para o VNA é utilizado um transceiver de rádio frequência para converter para banda base o sinal de rádio frequência e para converter para rádio frequência o sinal de banda base e uma FPGA para controlar o transceiver e para processamento. Foi criada uma interface para o utilizador recorrendo ao MATLAB® Graphical User Interface (GUI). Por fim, as medidas efectuadas por cada um dos sistemas implementados são discutidas. A potência medida pelo medidor de potência é comparada com os valores de referência. O osciloscópio é avaliado pelas figuras de mérito comuns e os parâmetros S medidos pelo VNA são comparados com os medidos por um VNA de referência.

Abstract

With the increase of available mobile network services, it is needed a more efficient management of resources. To accomplish that, accurate simulation tools and measuring equipments are required. The scientific community have proposed new equipments that allow a better characterization of Radio Frequency (RF) devices, as the VNAs. In this work some demonstrative measuring instruments are developed, using low cost and versatile/reconfigurable commercial components. The implemented instruments are a power meter, an oscilloscope and a VNA. For the power meter it is used a power detector and a FPGA to process and display the result. For the oscilloscope and VNA it is used a RF transceiver to down-convert the RF signal and up-convert the baseband signal and a FPGA to control the RF transceiver and processing. An user interface for oscilloscope and VNA was created using MATLAB® GUI. Lastly, the measurements performed by each one of the implemented systems are discussed. The power level measured by the power meter is compared with the reference values. The oscilloscope is evaluated by common respective figures of merit and the Scattering Parameters (S-parameters) measured by the VNA are compared with the ones measured by a reference VNA.

Contents

List of Figures

Acronyms

Γ	Reflection Coefficient
AC	Alternating Current
ADC	Analog-to-Digital Converter
DDS	Direct Digital Synthesizer
DUT	Device Under Test
DSP	Digital Signal Processing
DC	Direct Current
FFT	Fast Fourrier Transform
FPGA	Field Programmable Gate Array
FSM	Finite State Machine
GUI	Graphical User Interface
IF	Intermediate Frequency
LSNA	Large Signal Network Analyzer
LO	Local Oscillator
NVNA	Nonlinear Vector Network Analyzer
PLL	Phase Locked Loop
RF	Radio Frequency
RMS	Root Mean Square
SDK	Software Development Kit
S-parameters	Scattering Parameters
TIA	Trans-Impedance Amplifier
UART	Universal Asynchronous Receiver-Transmitter
VNA	Vector Network Analyzer
VSG	Vector Signal Generator

VSWR	Voltage Standing Wave Ratio
XADC	Xilinx Analog-to-Digital Converter
COTS	commercial of the shelf

Chapter 1

Introduction

1.1 Motivation

The services available through mobile communications are demanding better and better performances of the networks. This implies using the available resources more efficiently, since it is required to satisfy very restrictive rules with respect to the spectral use. To accomplish the imposed requirements, very good simulation tools and equipments capable of model accurately the RF devices are required. In the last years the scientific community have proposed measuring devices with new features compared to traditional power meters and oscilloscopes. The VNA, Nonlinear Vector Network Analyzer (NVNA) or Large Signal Network Analyzer (LSNA) are examples of the proposed instruments.

RF measuring instruments are usually very expensive. So, this thesis proposes to implement a demonstrative set of instruments using low-cost commercial of the shelf (COTS) components. With this work it is intended to disseminate the knowledge about the traditional architectures of some RF instruments and present architectures with some differences comparing with the traditional ones.

1.2 RF Lab

The instruments proposed to implement are three of the most used instruments on a RF lab, namely, RF power meters, oscilloscopes and VNAs. The commercial RF power meters are usually based on two main systems, the RF power detector and the processing system. The RF power detector outputs a voltage signal that can be converted by the processing system in the equivalent RF power of the input signal. The most used power detectors are thermal, or diode type.

There are two types of oscilloscopes, the real-time oscilloscopes and the equivalent-time sampling oscilloscopes. The real-time oscilloscopes acquire the waveform in a single trigger event. The equivalent-time sampling oscilloscopes use a sampling and hold circuit to acquire one sample at each trigger event. The equivalent-time sampling oscilloscopes have a higher bandwidth comparing with the real-time sampling oscilloscopes, with the disadvantage that are not able to capture single events of periodic signals.

The VNA is a measuring instrument designed to characterize/model RF devices or networks in frequency. The VNAs measure the incident and reflected waves at each port of a Device Under Test (DUT) and calculate the S-parameters.

The instruments described are some of the most used instruments in a RF lab. This work begins by describing this instruments and explaining its architecture. After to present the commercial instruments it is described how were implemented low cost versions of each one of them.

There are some works made with the objective of implementing RF measuring instruments, one of them is [1] that implemented a VNA. This thesis presents better results of S_{11} parameters phase of one-port devices comparing with the [1], and similar results for the rest of the S-parameters.

1.3 Document Overview

The **Chapter 1** introduces the dissertation.

In **Chapter 2** the most common architectures of commercial power meters, oscilloscopes and VNAs are explained. Relatively to power meters, are presented the technologies used to measure the power and a traditional architecture of a power meter. Relatively to oscilloscopes are explained the two types of sampling commonly used and the traditional architectures of digital oscilloscopes are presented. The specifications usually defined for oscilloscopes are also presented. After that, the S-parameters are introduced, the VNA architecture is explained and its calibration is also explained.

Chapter 3 starts by describing the equipments used, and explaining the reason for its choice. After that it is presented the architecture of the implemented instruments.

In **Chapter 4** the entire calibration process that was implemented on VNA is described.

Chapter 5 is the chapter where the results of each one of the implemented instruments are exposed and explained. In the power meter case, it is presented the values of the measured power and comparing it to a reference instrument. For oscilloscope is presented the graphical user interface and the voltage waves measured. Finally, for the VNA is also

presented its graphical user interface, the S-parameters measured and the errors associated.

The **Chapter 6** presents the final conclusions and makes some suggestions to further improve the work.

Chapter 2

RF Lab Instruments

2.1 Introduction

Since the beginning of electronics there has been a major necessity of measuring and characterizing electronic circuits, so over the years several instruments designed with that purpose have emerged. The first of these instruments had the objective of measuring waves in circuits as voltage and current or measuring its power (oscilloscopes and power meters). With the frequency increasing, the need for characterizing the behaviour of electronic devices in frequency has grown, so instruments for that purpose were created. The mostly used one is the VNA. The VNA and similar instruments calculate the S-parameters, which characterize the linear behaviour of a device in a point of frequency.

More recently with the need of more efficient devices and systems they have been increasingly pushed to the nonlinear zone and their characterization with a linear model has become poor, so instruments to obtain nonlinear models of the devices were developed, as NVNA, and LSNA [2].

This chapter starts by describing the traditional architecture of power meters, then it is explained the architecture of an oscilloscope and lastly is exposed the VNA/NVNA architecture also explaining the S-parameters.

2.2 RF Power Meters

The instrument responsible for measuring RF power is named RF Power Meter. Its typical architecture, illustrated by figure 2.1, is composed by two main blocks, the power detector and the power meter base module. The power detector receives RF signal and outputs a proportional Direct Current (DC) voltage. The power meter base module am-

plifies and digitizes the DC voltage, converts it in power and displays the result [3]. There are different architectures for power meters, as the receiver based power meter, which is not explained in this thesis.

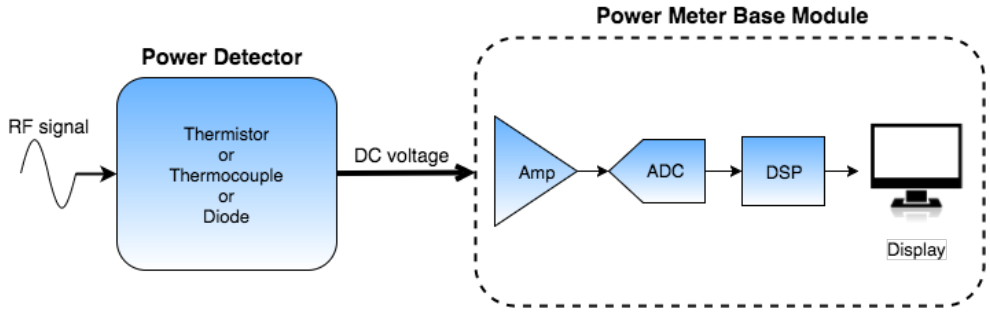

Figure 2.1: Power Meters Simplified block diagram

The power detector is usually based on diodes or thermal elements, as thermistors or thermocouples. Thermistor is a temperature-sensitive resistor and is usually placed on a self-Balancing Wheatstone bridge to easily measure the resistivity change and calculate the RF power [4]. Thermocouple is a junction of two dissimilar metals. When the junction is heated, it creates a voltage drop that depends on the two metals and the temperature of the junction, this phenomenon is known as the Seebeck effect. Briefly, diode-based power meters use diodes to rectify the RF signal. After rectification the signal can be filtered obtaining this way a DC voltage that can be related to the power of the RF signal [5].

2.3 Digital Oscilloscope

Digital oscilloscopes were created to rectify several of the negative aspects of the analogue oscilloscopes. The digital oscilloscopes can be divided into two categories: the real-time oscilloscopes and the equivalent-time sampling oscilloscopes [6]. The real-time and the equivalent-time sampling oscilloscopes are based in different sampling principles, which are explained in the following sections. The equivalent-time oscilloscopes have much higher bandwidths than the real-time oscilloscopes but they can only measure periodic signals, while real-time oscilloscopes can measure single shot events.

2.3.1 Types of measurements

Because of the available processing power coupled with the mass storage capability existent nowadays, the digital oscilloscopes are capable of performing a variety of functions

beyond which the oscilloscopes that were created in the first place. Nowadays digital oscilloscopes are usually capable of providing [7]:

- Real time or stored waveform display
- Accurate time and voltage measurement using cursors
- Digital display of voltage and frequency and/or periodic time
- Accurate measurement of phase angle
- Frequency spectrum display and analysis
- Capability to export stored waveform data
- Capability to save/print waveforms and other information in graphical format

2.3.2 Real-time Oscilloscope

A typical real-time block diagram is illustrated in figure 2.2. The input signal is scaled by the attenuator and pre-amplifier, then it is digitized and the acquisition processor decides what data should be saved and processed based on the information given by the trigger control. The display processor and the display are responsible for processing and displaying the intended data.

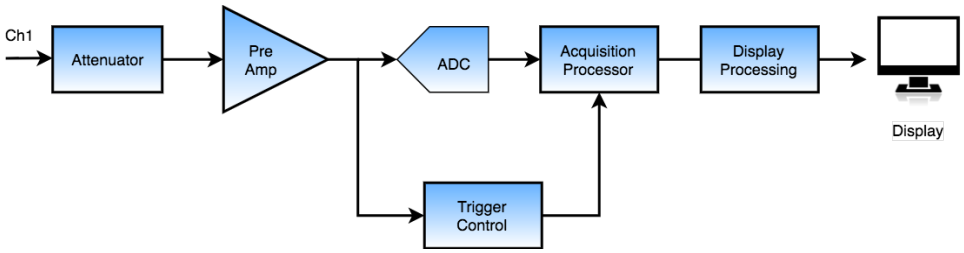

Figure 2.2: Real-time Oscilloscope Simplified block diagram

The functions of an oscilloscope which require more attention are sampling and trigger. The real-time oscilloscope samples an entire waveform in a single trigger event. The sample clock defines the instants that the Analog-to-Digital Converter (ADC) takes a sample, and in a single shot enough samples are taken to fully reconstruct the waveform. Hence it is required the ADC to be fast enough to satisfy the Nyquist Rule, which states that the sampling frequency must be at least twice as high as the maximum frequency component of the signal. Since the ADCs sampling rate is limited, the waveform the oscilloscope is

able to measure correctly is also frequency limited. There are several trigger types but the most common ones are the rising edge trigger, the falling edge trigger and the falling and rising edge trigger. If the oscilloscope is triggered in rising edge, when the incoming waveform amplitude reaches the trigger level defined the scope starts converting it. The trigger provides a horizontal time reference point for the incoming data [8]. The waveform acquisition using a real-time oscilloscope is illustrated by figure 2.3.

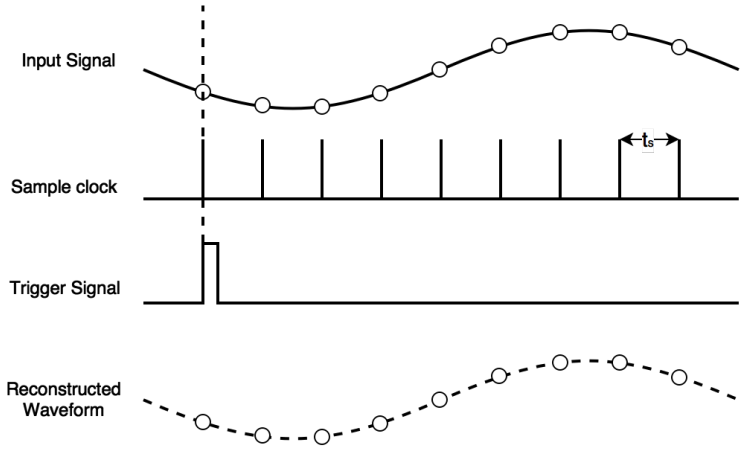

Figure 2.3: Waveform acquisition using a real-time Oscilloscope

2.3.3 Equivalent-time Sampling Oscilloscope

The equivalent-time sampling oscilloscopes were created to achieve higher bandwidth than the real-time oscilloscopes. The typical block diagram of an equivalent-time sampling oscilloscope is illustrated by figure 2.4. The main differences from the real-time oscilloscope are in the sampling process. It is used a sample and hold circuit controlled by the acquisition processor, and right after that its output voltage is amplified and digitized [6].

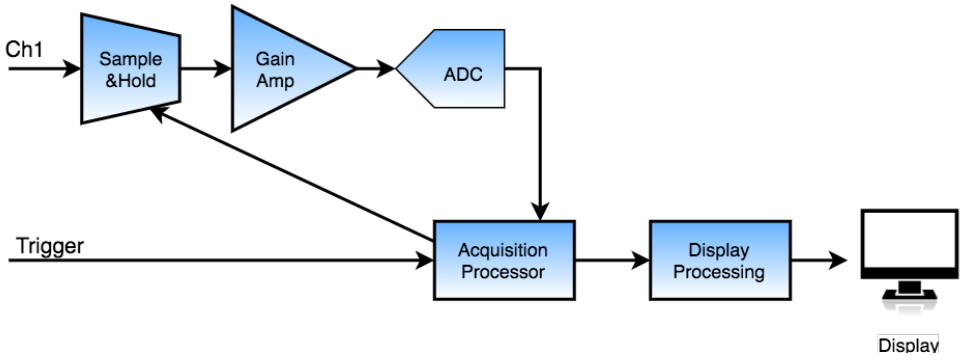

Figure 2.4: Real-time Oscilloscope Simplified block diagram

In the equivalent-time sampling only one sample is taken per trigger cycle, hence the number of samples intended determines the number of trigger cycles to reproduce a waveform. The frequency response of the sampler settles the measurement bandwidth, in other words the faster the sampler is, the higher the bandwidth that is achieved. The waveform acquisition using an equivalent-time sampling oscilloscope requires a trigger synchronous with the input signal, usually provided by the user. After a sample is taken the trigger is armed and a precise incremental delay is added before taking the next sample. This process is repeated until all required samples are taken, the incremental delay is determined by the time base setting as well as the number of points [8]. The entire sampling process is described by figure 2.5.

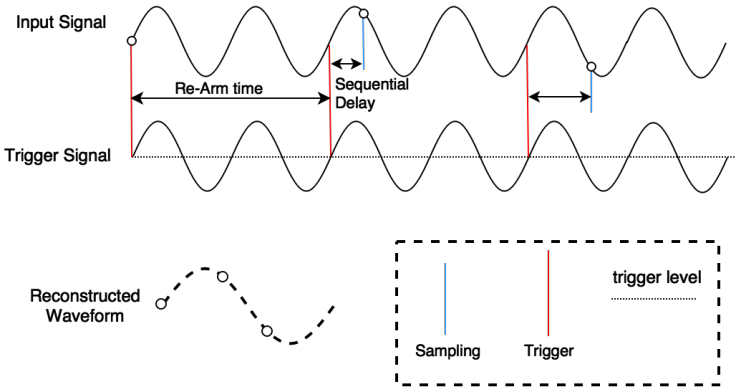

Figure 2.5: Waveform acquisition using a equivalent-time sampling Oscilloscope

2.3.4 Specifications

Every instrument or device has to be characterized for the user to know its behaviour. Each instrument or device, has an ordinary set of specifications, which should be defined for the user to know if it is adequate to use it in some application. The oscilloscope specifications can be divided by system. In the current section the digital oscilloscope specifications are presented and explained.

Vertical System

The vertical system specifications that are usually defined by the manufacturers are Bandwidth/rise time, Vertical (DC) gain Accuracy, Offset accuracy, Resolution, Dynamic range.

- **Bandwidth/rise time**

The bandwidth defines the frequency range of signals that the oscilloscope is capable of measuring and displaying accurately. The electrical bandwidth is defined by the IEEE 1057 standard [9] as the point at which the amplitude of a sine wave is attenuated by 3 dB comparing to its power at a lower reference frequency. The bandwidth that an oscilloscope should have to correctly display a signal (max of 2% of error) is five times higher than the frequency of the signal. The rise time, or step response depends directly on the bandwidth. Oscilloscopes with higher bandwidth have faster dynamics and consequently smaller rise times. In real-time oscilloscopes, the relation between bandwidth and rise time is around: Bandwidth x Rise time = 0.45. [10].

- **Vertical (DC) gain and Offset Accuracy**

  The vertical gain accuracy is the accuracy of the gain applied to the input voltage. It is important to determine accurately the input voltage or when two signals are compared with different gains applied. The vertical gain is usually expressed as a percentage of full scale voltage. The offset accuracy is the accuracy that the offset added or subtracted to the signal appearing on the screen.

- **Resolution and Dynamic Range**

  The dynamic range of an oscilloscope is the maximum input voltage divided by the minimum input voltage possible to be measured. The resolution of an oscilloscope expresses the granularity of the digitalization, it depends on the ADC number of bits and the dynamic range of the oscilloscope [10].

Horizontal System

The most important piece of the horizontal system is the sample clock. Its characteristics define the key specifications of the horizontal system, which are the sample rate, the sample rate accuracy and the Delta-time measurement accuracy.

- **Sample rate and Sample rate accuracy**

  The sample rate of any digital oscilloscope is settled by a clock, called sample clock. The waveform reconstruction depends on the uniform time intervals between the sample points, so the sample clock accuracy is crucial to get accurate measurements. The clock accuracy is defined by the long-term sample rate accuracy, expressed in parts per milion (PPM) and delay time accuracy is usually expressed in milliseconds (ms) [10].

- **Delta-time measurement accuracy**

  In oscilloscopes that use very high clock rates accurate time interval (delta-time) measurements become important when characterizing setup and hold time, skew and jitter. For single-shot timing measurements delta-time accuracy is the most important specification, because it defines the maximum error of the timing measurements. Delta-time accuracy is based on factors as timebase accuracy, sample interval and the aggregate performance of the entire digitizing system [10].

Acquisition System

The acquisition system depends highly on the time base clock. As previously explained, the Acquisition system main functions are digitization and storage of the waveform. The key specifications of the acquisition system are record length and waveform capture rate.

- **Record length** The record length is the number of points that an oscilloscope can store for one waveform. The record length determines the time duration that can be acquired at a given sample rate according to the following expression [10]:

$$Duration(s) = \frac{Recordlength(samples)}{SampleRate(samples/s)} \tag{2.1}$$

- **Waveform capture rate** The waveform capture rate is the rate at which the waveform is updated and is expressed in waveforms per second (wfms/s). The capture rate is given by:

$$Capture_{rate}(wfms/s) = \frac{1(wfms)}{Acquisitiontime(s) + SystemHoldoffTime(s)} \tag{2.2}$$

  Where the system hold-off time is the time during which the instrument processes the acquired data, resets the system and waits for the next trigger event.

  Based on the waveform capture rate it is possible to calculate the probability of capturing an infrequent event:

$$Probabilityofcapture = \frac{Acquisitiontime(s)}{Acquisitiontime(s) + SystemHolfoffTime(s)} \tag{2.3}$$

  This probability of capture is only valid for real-time oscilloscopes, because the equivalent-time sampling oscilloscopes were designed just to measure stationary waveforms [10].

Trigger System

The trigger system sets the point at which the ADC should start digitizing the waveform, so the trigger performance determines what can be captured, viewed and measured by the oscilloscope. The most important trigger specifications are Sensitivity, Trigger coupling, Jitter and Trigger Type.

- **Sensitivity**

  The trigger sensitivity determines the capacity of an oscilloscope to react to a specified edge trigger conditions over a range of frequencies. The trigger sensitivity specifies the range of frequencies and the minimum signal amplitude, in display divisions that are required for the oscilloscope to detect and trigger the waveform. The trigger sensitivity is specified with a sine wave input [10].

- **Trigger coupling**

  The oscilloscope trigger coupling allows the user to set the trigger under different signal and noise conditions. The most common coupling modes are the DC coupling and Alternating Current (AC) coupling. The DC coupling considers all of the signal frequency components for trigger. The AC coupling filters the low frequency components (usually below 100Hz), considering only the non-filtered components for the trigger.

- **Trigger Jitter**

  Trigger Jitter is the deviation from the instant that the trigger should be performed and the instant that it is actually performed.

  The stability and accuracy of the trigger system depends on the jitter, especially in the sampling oscilloscopes. To get precise and stable waveform it is required to have a small jitter. The jitter is expressed in time units (seconds).

- **Trigger type**

  There are a big variety of trigger types. They can be divided in two categories: the edge trigger and the advanced trigger. The most used ones are the edge trigger, which can be a positive or negative edge, and the voltage threshold can be defined by the user. The advanced trigger types perform several different functions that will not be discussed in this thesis.

2.4 VNA

In electronics, every device needs to be characterized so that the engineers who use it know its behaviour and are able to use it correctly. For RF device modeling, as for example antennas, filters or power amplifiers, RF engineers are used to employ the S-parameters. The mostly used instrument to calculate the S-parameters is the VNA [11]. In this section, the S-parameters are explained, then the VNA architecture is exposed explaining its functioning and lastly the calibration process that is required to get reliable measurements is described.

2.4.1 S-Parameters

The S-parameters are the ratios between the spectral power at the intended frequency of the scattered and incident waves at the ports of a microwave device or circuit. The figure 2.6 represents a two-port device, with the incident and reflected waves at both ports and the S-parameters.

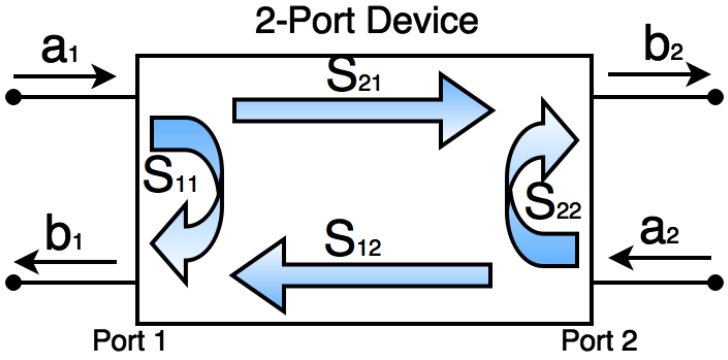

Figure 2.6: Representation of S-parameters in a two port device

According to the [11], the S-parameters expressions for two port devices are:

$$S_{11} = \left.\frac{b_1}{a_1}\right|_{a_2=0} \tag{2.4}$$

$$S_{21} = \left.\frac{b_2}{a_1}\right|_{a_2=0} \tag{2.5}$$

$$S_{12} = \left.\frac{b_1}{a_2}\right|_{a_1=0} \tag{2.6}$$

$$S_{22} = \left.\frac{b_2}{a_2}\right|_{a_1=0} \tag{2.7}$$

where a_i and b_i are the incident and reflected waves respectively at port i.

The S_{21} and S_{12} parameters are the forward and reverse gain when the incident waves at port 2 and port 1 are equal to zero respectively. The S_{11} parameter is the reflection coefficient at port 1 when the incident wave at port 2 is equal to zero and the S_{22} parameter is the reflection coefficient at port 2 when the incident wave at port 1 is equal to zero [11].

2.4.2 Traditional Architecture

The most common VNA architecture is the two-port architecture illustrated by figure 2.7. The VNA architecture is composed by one signal generator, two directional couplers, two microwave receivers, one processor and one display [12] .

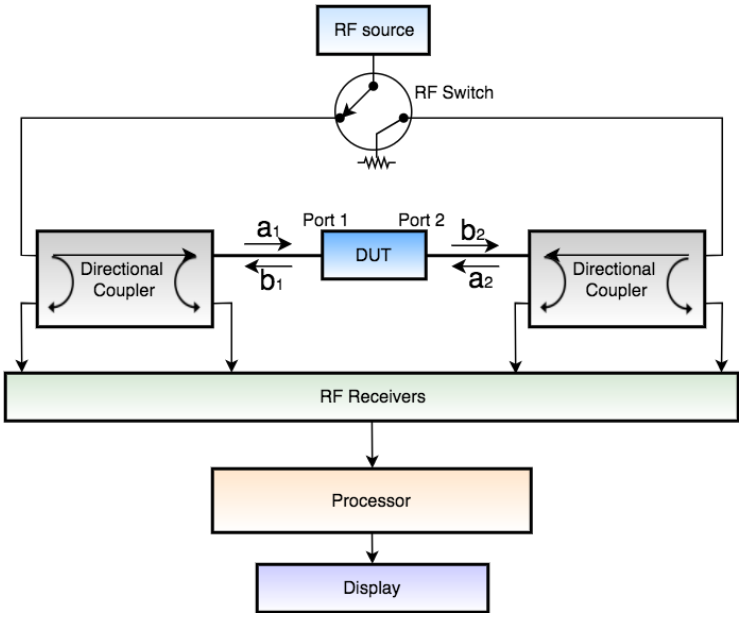

Figure 2.7: Simplified block diagram of a VNA

Signal Generator

A two-port VNA can have one or two signal generators. In the case of having just one, as the figure 2.7 shows, a switch must be used to make it possible to excite alternately port 1 and port 2 of the DUT. The signal generators should allow sweeping the frequency and the power of the signal generated [11].

Directional couplers

A directional coupler is a four-port passive device whose objective is to separate the incident and reflected traveling voltage waves. The figure 2.8 illustrates a block diagram of a directional coupler. The directional couplers are placed one at each DUT port; the input port of the directional couplers is connected to the RF signal generator and the Through port of the directional couplers is connected to port 1 and port 2 of the DUT. Most of the power injected at the Input port of the coupler appears at the Through port and a fraction of the same injected power appears at the Coupled port [11].

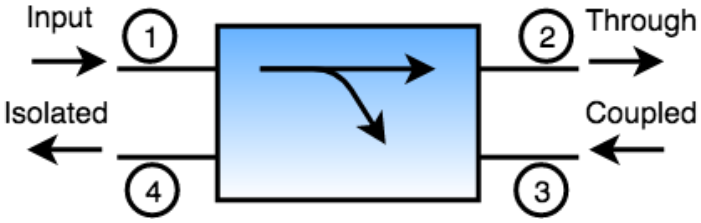

Figure 2.8: Directional Coupler block diagram

The injected power at the input port (P_1) and the output power at the coupled port (P_3) are related by the coupling (C), according to the [11]:

$$C = 10log(\frac{P_1}{P_3}) \tag{2.8}$$

The isolation (I) relates the injected power at the input port (P_1) and the output power at the isolated port (P_4). In ideal case P_4 is equal to zero and the isolation is infinite [11].

$$I = 10log(\frac{P_1}{P_4}) \tag{2.9}$$

Using the coupling and the isolation, the power applied to the DUT can be measured. The scattered wave can also be measured with a directional coupler. In this case for the scattered wave, port 2 is the input port, port 3 is the isolated port and port 4 is the coupled port. Another figure of merit of a directional coupler is directivity, which is the capacity of separating the incident and reflected waves, and is defined by the following expression [11].

$$D = 10log(\frac{P_3}{P_4}) \tag{2.10}$$

The three figures of merit defined above are related by the following expression:

$$I = D + C \tag{2.11}$$

Microwave Receivers

The receivers are the most important blocks in a VNA. They measure the amplitude and phase of the incident and scattered traveling waves at both ports of the DUT. The receivers architecture is based on the superheterodyne principle, where the RF signal is down-converted to an Intermediate Frequency (IF) mixing the input signal with the LO. After the signal is at IF, it is amplified and band-pass filtered to remove unwanted spectral components mainly created by the mixer and hence improving the dynamic range and the sensitivity. After the filtering the signal is digitized by the ADC. In early configurations instead of using an ADC, the amplitude of the signal was measured using an envelope detector and the phase using a quadrature detector. To measure both incident and scattering traveling waves two receivers must be used and the sampling should be synchronous to measure the relative phase between the two measured waves [11].

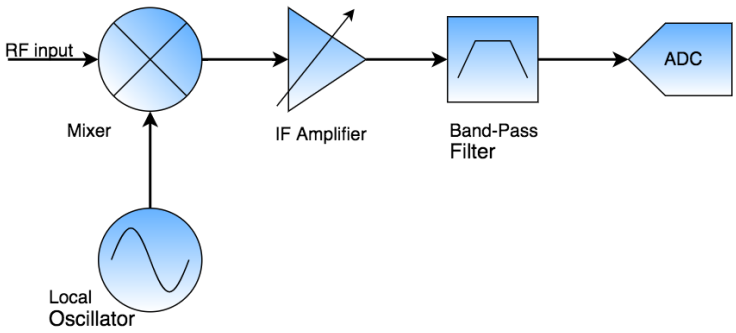

Figure 2.9: The receiver of a VNA

DSP and Display

The Digital Signal Processing (DSP) is what processes stores and performs the required calibrations. The S-parameters are displayed usually in a rectangular graph or in a smith chart, depending on the user's choice.

2.4.3 Calibration Procedure

Any RF or microwave measurement instrument is non-ideal as there are always systematic errors introduced as losses and phase shifts in the cables, imperfections of the directional couplers, mismatches, etc. Hence, the measured waves are different from the waves that are actually present at the DUT ports. The calibration procedure aims to remove the systematic erros by building a error model and calculate the errors associated

to each measure. To calculate the parameters of the error model, there are measured well known devices and it is used the measured response and the theoretical one [11].

In the model of 2.12 the measured waves instantiated by the subscript R are different from the waves that we are interested in, instantiated by the subscript D. The relationship between the measured waves and the waves present in the DUT can be expressed by the equation 2.12, according to [11]:

$$\begin{bmatrix} a_{1i}^D \\ b_{1i}^D \\ a_{2i}^D \\ b_{2i}^D \end{bmatrix} = \begin{bmatrix} \alpha_{1i}^{'} & \beta_{1i}^{'} & 0 & 0 \\ \gamma_{1i}^{'} & \delta_{1i}^{'} & 0 & 0 \\ 0 & 0 & \alpha_{2i}^{'} & \beta_{2i}^{'} \\ 0 & 0 & \gamma_{2i}^{'} & \delta_{2i}^{'} \end{bmatrix} \begin{bmatrix} a_{1i}^R \\ b_{1i}^R \\ a_{2i}^R \\ b_{2i}^R \end{bmatrix} \tag{2.12}$$

where i is the frequency index.

The calibration's objective is to determine the unknown matrix coefficients. As it can be seen in 2.12, 8 of the 16 matrix coefficients are equal to zero. This simplification was made assuming no coupling between port 1 and port 2 of the DUT. This assumption is usually valid for connectorized measurements because the distance between the different ports is enough for the coupling to be negligible. Since the S-parameters are the ratio of two waves, all matrix coefficients can be divided by one of them without affecting the S-parameters value. This way only seven coefficients remain to calculate because one of them is equal to one [11].

The equation 2.13 presents the simplifications described above.

$$\begin{bmatrix} a_{1i}^D \\ b_{1i}^D \\ a_{2i}^D \\ b_{2i}^D \end{bmatrix} = \alpha_{1i}^{'} \begin{bmatrix} 1 & \beta_{1i} & 0 & 0 \\ \gamma_{1i} & \delta_{1i} & 0 & 0 \\ 0 & 0 & \alpha_{2i} & \beta_{2i} \\ 0 & 0 & \gamma_{2i} & \delta_{2i} \end{bmatrix} \begin{bmatrix} a_{1i}^R \\ b_{1i}^R \\ a_{2i}^R \\ b_{2i}^R \end{bmatrix} \tag{2.13}$$

To calculate the unknown parameters of the equation 2.13,a calibration procedure is required. There are several calibration standards such as short-open-load-thru (SOLT), thru-reflect-load (TRL) or load-reflect-match (LRM) [2] .

In the current thesis, the SOLT calibration is explained because it is the most commonly used for connectorized measurements and due to its simplicity and accuracy.

To perform the SOLT calibration each one of the three one-port standards (Short, Open and Load) should be applied to each one of the VNA's ports, and the two ports should be interconnected with the "Thru" standard.

The standards are not perfect, and the manufacturer supplies the necessary information to calculate the Reflection Coefficient (Γ) of each one of the standards. Later in this chapter, it is explained what are the parameters commonly supplied and how Γ can be calculated for each one of the standards.

The relations between the incident and reflected traveling voltage waves are:

$$\Gamma_i^O a_{1i}^{D1} = b_{1i}^{D1} \tag{2.14}$$

$$\Gamma_i^S a_{1i}^{D2} = b_{1i}^{D2} \tag{2.15}$$

$$\Gamma_i^L a_{1i}^{D3} = b_{1i}^{D3} \tag{2.16}$$

$$\Gamma_i^O a_{2i}^{D4} = b_{2i}^{D4} \tag{2.17}$$

$$\Gamma_i^S a_{2i}^{D5} = b_{2i}^{D5} \tag{2.18}$$

$$\Gamma_i^L a_{2i}^{D6} = b_{2i}^{D6} \tag{2.19}$$

The superscript number 1 to 6 numbers the measurement that should be performed and the superscripts O, S, and L stand for Open, Short and Load respectively. Using the equation 2.13, the DUT waves can be replaced by the measured quantities as it follows:

$$\Gamma_i^O(a_{1i}^{R1} + \beta_{1i} b_{1i}^{R1}) = \gamma_{1i} a_{1i}^{R1} + \delta_{1i} b_{1i}^{R1} \tag{2.20}$$

$$\Gamma_i^S(a_{1i}^{R2} + \beta_{1i} b_{1i}^{R2}) = \gamma_{1i} a_{1i}^{R2} + \delta_{1i} b_{1i}^{R2} \tag{2.21}$$

$$\Gamma_i^L(a_{1i}^{R3} + \beta_{1i} b_{1i}^{R3}) = \gamma_{1i} a_{1i}^{R3} + \delta_{1i} b_{1i}^{R3} \tag{2.22}$$

$$\Gamma_i^O(a_{2i}^{R4} + \beta_{2i} b_{2i}^{R4}) = \gamma_{2i} a_{2i}^{R4} + \delta_{2i} b_{2i}^{R4} \tag{2.23}$$

$$\Gamma_i^S(a_{2i}^{R5} + \beta_{2i} b_{2i}^{R5}) = \gamma_{2i} a_{2i}^{R5} + \delta_{2i} b_{2i}^{R5} \tag{2.24}$$

$$\Gamma_i^L(a_{2i}^{R6} + \beta_{2i} b_{2i}^{R6}) = \gamma_{2i} a_{2i}^{R6} + \delta_{2i} b_{2i}^{R6} \tag{2.25}$$

with:

$$\beta_{2i}^{''} = \frac{\beta_{2i}}{\alpha_{2i}} \tag{2.26}$$

$$\gamma_{2i}^{''} = \frac{\gamma_{2i}}{\alpha_{2i}} \tag{2.27}$$

$$\delta_{2i}^{''} = \frac{\delta_{2i}}{\alpha_{2i}} \tag{2.28}$$

From equation 2.20 to equation 2.25 six equations are enunciated to calculate the seven unknown parameters. The "Thru" standard provides the last equation:

$$a_{1i}^{D7} = b_{2i}^{D7} \tag{2.29}$$

From 2.13 and 2.29 results:

$$a_{1i}^{R7} + \beta_{1i} b_{1i}^{R7} = \alpha_{2i}(\gamma_{2i}^{''} a_{2i}^{R7} + \delta_{2i}^{''} b_{2i}^{R7}) \tag{2.30}$$

Now the seven parameters can be calculated and the calibration process is finished.

Calibration Standards

The SOLT calibration requires four standards: Short, Open, Load and "Thru". In this section each of them will be explained.

The short standard is as close as possible of an ideal short, ideally the reflection coefficient modulus $|\Gamma|$ would be equal to 1. In the coaxial design there is always an offset length l between the reference plane and the short plane, making Γ dependent on the l [12]. Hence the Γ can be written as:

$$\Gamma = -e^{-2(\alpha + j\beta)l} \tag{2.31}$$

Where α is the attenuation constant expressed in nepers per meter (Np/m) and β is the phase constant expressed in radians per meter (rad/m).

The α represents the attenuation of the electromagnetic wave along the cable and β represents the phase change per meter [12].

The attenuation due to the offset length (α) is negligible and the phase shift is imposed by the length of the standard, so Γ can be written as:

$$\Gamma = -e^{-4\pi l/\lambda} \tag{2.32}$$

where

$$\beta = \frac{2\pi}{\lambda} \tag{2.33}$$

and

$$\lambda = \frac{c}{f} \tag{2.34}$$

where c is the speed of light in vacuum and f is the operation frequency. For the short standard, Γ can also be defined by the parasitic inductances. The frequency dependent parasitic inductance $L(f)$ is usually defined as:

$$L(f) = L_0 + L_1 f + L_2 f^2 + L_3 f^3 \tag{2.35}$$

So Γ can be written as:

$$\Gamma^S = \frac{j2\pi f L(f) - Z_0}{j2\pi f L(f) + Z_0} e^{-j4\pi l/\lambda} \tag{2.36}$$

The coaxial open standard is a closed design, to avoid radiation effects at the end of the inner conductor. In a closed design, a frequency dependent capacitance is formed at the open end of the inner conductor [12]. This capacitance can be approximated by the following third order expression:

$$C(f) = C_0 + C_1 f + C_2 f^2 + C_3 f^3 \tag{2.37}$$

The Γ for the open standard depends on the parasitic capacitance and the offset length from the reference plane to the open end of the inner conductor, and it is given by:

$$\Gamma^O = \frac{1 - j2\pi f Z_0 C(f)}{1 + j2\pi f Z_0 C(f)} e^{-j4\pi l/\lambda} \tag{2.38}$$

The load standard has a broadband impedance that ideally must match with the system impedance. However, some VNAs allow to introduce some non-ideal properties of the load [12].

The "Thru" standard is a direct connection between the two ports.

Chapter 3

Implemented Architectures description

3.1 Overview

This chapter starts by presenting the used material to implement the power meter, the oscilloscope and the VNA. For all material used the relevant specifications for its application on this thesis are presented. After that the power meter, the oscilloscope and the VNA are described.

3.2 Used Material Description

3.2.1 FPGA

To implement the proposed instruments, it was required a core device versatile enough to be used in all of them, so a FPGA ZC706 Evaluation Board from Xilinx was used. Beyond the usual programmable hardware this FPGA provides a dedicated Zinq processor, a Xilinx Analog-to-Digital Converter (XADC) and is compatible with RF transceivers. The used FPGA provides a much bigger quantity of functions and peripherals that will not be used in this thesis [13].

3.2.2 Transceiver

Except for the power meter, the proposed instruments require a RF transceiver. The used RF transceiver is the AD9371 Evaluation Board from Analog Devices. This transceiver

provides a dual-channel receiver and a dual-channel transmitter. It operates over a frequency range of 300 MHz to 6 GHz and can transmit signals with bandwidths up to 250 MHz and receive signals with bandwidths up to 100 MHz [14].

The high bandwidth presented by this transceiver was the main reason for its choice.

3.2.3 Directional Couplers

The VNAs should measure the incident and reflected waves in each port of a DUT. The devices responsible for separate the incident and reflected voltage traveling waves are the directional couplers. Directional couplers from Mini-Circuits with reference (ZGBDC20-33HP+) were used. It operates in the frequency range from 300 MHz to 3000 MHz, that limits the frequency range of the transceiver. It presents a typical Directivity of 24 dB and a typical Coupling of 22.2 ± 0.4 dB in the frequency range of 2000MHz to 3000MHz that is the frequency range that it will be used in this work [15].

3.2.4 Isolators

The used isolators were the Narda isolators, model 4913. These isolators are designed to work from 2 GHz to 4 GHz and within the temperature range of 0 to 55 degrees Celsius. Its minimum isolation is 18 dB, the maximum Insertion Loss is 0.5 dB and the maximum Voltage Standing Wave Ratio (VSWR) is 1.30. In terms of power, the peak power is 50 watts, and the average power is 25 watts for forward and 1 watt for reverse [16].

Although its frequency range limits the frequency range of the setup, these isolators have good characteristics and a pair of them was available on the RF laboratory.

3.2.5 Power Detector

The power detector used for the power meter is the demo 1599A from Linear Technology. The 1599A is the demo board of the power detector LTC5583 that is a Matched dual-channel 6 GHz power detector. Although the LTC5583 has a frequency range from 40 MHz to 6 GHz its demo board is set up for 40 MHz to 3 GHz operation.

The main reason for choosing the referred power meter is the frequency range. Beyond its frequency range, the power detector has a dynamic range up to 60 dB and is able to measure accurately several RF standards [17].

3.2.6 Vector Signal Generator

Despite the RF transceiver has internal Phase Locked Loops (PLLs) that can be used to generate the LO to perform the down-conversion and up-conversion of the RF signal, it was used external LO.

The LO frequency is generated by a Vector Signal Generator (VSG). The VSG used is the SMU 200A from Rohde & Schwarz. Its frequency range is 100kHz to 6GHz [18].

3.3 Power Meter

Similarly to the commercial power meters, the implemented architecture illustrated by figure 3.1, is composed by a power detector, an ADC, a processor and a display.

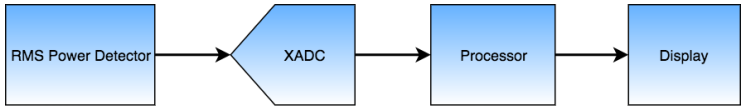

Figure 3.1: Block diagram of the implemented power meter

The power detector outputs a voltage proportional to the RF Root Mean Square (RMS) signal power. The output voltage of the power detector, is digitized by the XADC of the FPGA, then is converted to RMS power by the processor of the FPGA according to the manufacturer calibration indications and the signal power is printed. The power detector used outputs an output voltage between 0 V and 2.5 V and the XADC supports differential input voltages with maximum amplitude of 1 V. To convert the power detector's output voltage in a voltage within the input range of the XADC was used a voltage divider.

Figure 3.2 illustrates the setup used for power meter.

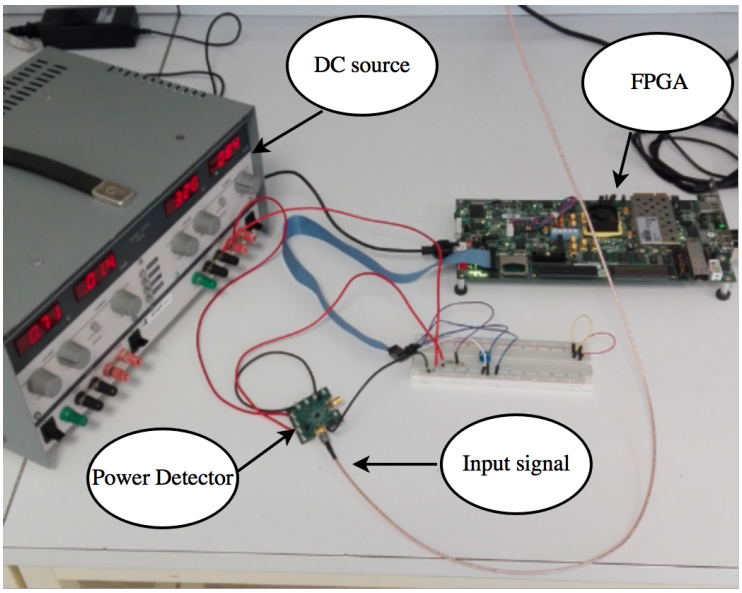

Figure 3.2: Setup of the implemented power meter

3.4 Oscilloscope

The implemented oscilloscope architecture is illustrated by figure 3.3.

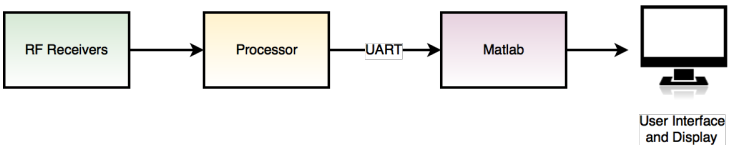

Figure 3.3: Simplified Block diagram of the implemented oscilloscope

The data acquisition is made by the RF transceiver, the FPGA is responsible for controlling the transceiver and save the sampled data, the data is sent to MATLAB® through Universal Asynchronous Receiver-Transmitter (UART). The oscilloscope interface was built using the MATLAB® GUI. Each one of the systems of the figure 3.3, is explained in more detail in the next sections.

Figure 3.4 illustrates the setup used for the oscilloscope.

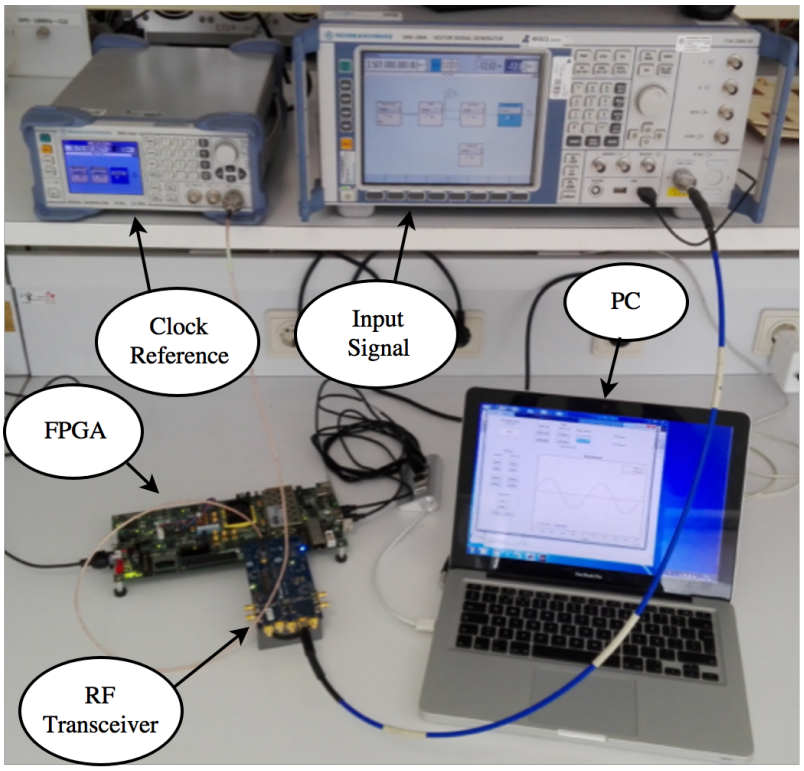

Figure 3.4: Setup of the implemented oscilloscope

3.4.1 RF Receivers

The traditional oscilloscopes architectures are based in real-time sampling or equivalent-time sampling oscilloscopes as described in chapter 2. The receiver of the implemented oscilloscope uses mixers to down-convert the RF signal and samples the signal in baseband. The oscilloscope uses the Rx channels of the RF transceiver, that follow the architecture described on figure 3.5.

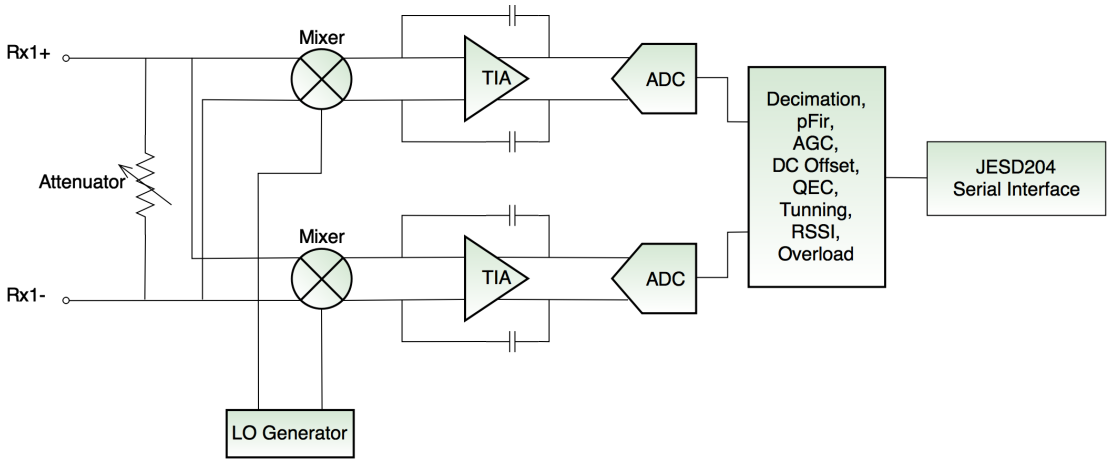

Figure 3.5: Block diagram of the main receivers of the RF transceiver used (AD9371)

As shown in figure 3.5, the receivers are differential. The signal is first attenuated by one attenuator that is controlled by software and allow two operation modes, automatic gain control or manual gain control. In manual gain control, the attenuation/gain is settled to one value and remains fixed.

After attenuated, the signal is down-converted by mixers. The LO is generated by the clock generator AD9528 that is integrated in the RF transceiver used. The mixers output signal is amplified by the Trans-Impedance Amplifier (TIA) and then is digitized by 16 bits ADCs. Once the signal is in digital domain, it is processed by several blocks. These blocks perform filtering, attenuations, DC offset correction, quadrature error correction. It also read the received signal strength indicator and detects if overload has occured.

The signal is transferred to the FPGA by JESD204B interface. The JESD204B interface is a serial interface designed to reach high speed rates up to 12.5 Gbps.

3.4.2 Processor

The FPGA used for the oscilloscope is the same used for the power meter. All the required hardware to operate the transceiver is programmed in the FPGA, so it controls the transceiver and allow all necessary signal processing using its integrated Zinq processor, that is programmed through Software Development Kit (SDK).

For the oscilloscope, the FPGA communicates with MATLAB® using an UART to receive information about the central frequency in which the user desired to measure the signal and send the measured waveforms. For the communications to flow correctly a state machine was created in both MATLAB® and FPGA.

3.4.3 MATLAB®

The MATLAB® is responsible for receive and display the waveforms. The waveforms are displayed through a MATLAB® GUI, that also allow the user to adjust the necessary parameters to correctly visualize the desired waveform.

With the used setup it was not possible to implement the trigger system and the horizontal system as it is usually implemented. Instead of having a dedicated system to determine the instant that the ADC should start sampling the waveform, the implemented oscilloscope starts sampling as fast as the system allows and the MATLAB® analyze the received waveform, determines the point that the system should trigger and drop the excess of sampled points. The amplitude scaling is also performed by the MATLAB®, unlike the conventional oscilloscopes that scale the input waveform using an amplifier.

3.5 VNA

The architecture of the implemented VNA is illustrated by figure 3.6.

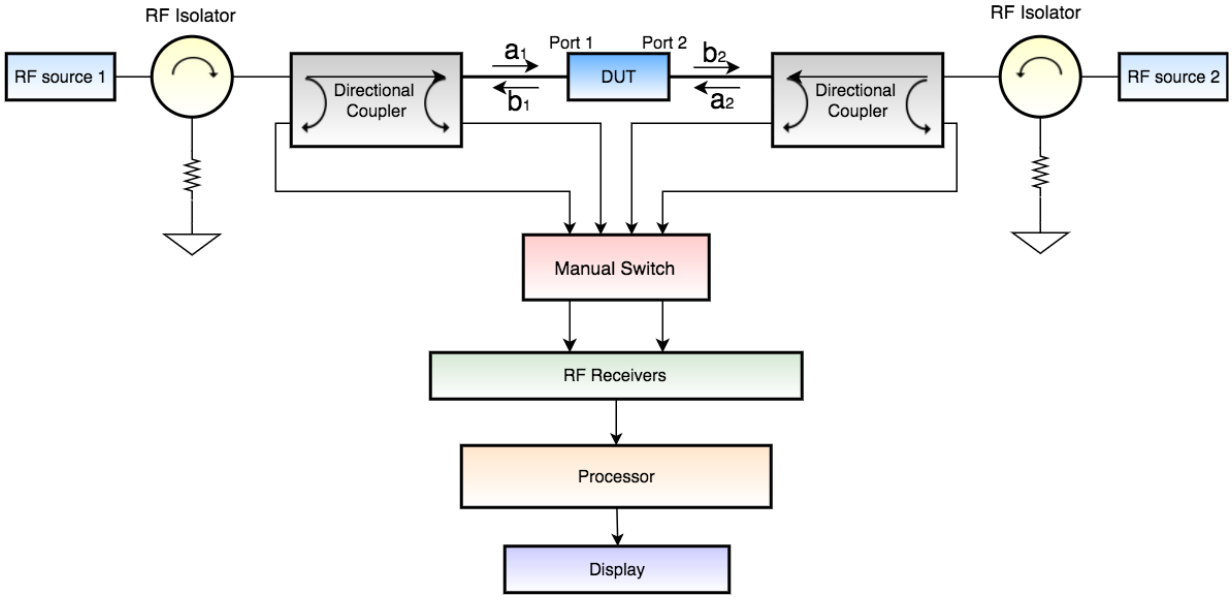

Figure 3.6: Block diagram of the implemented VNA

The RF source 1 and RF source 2 are the two transmitters of the RF transceiver. This way the DUT can be excited in port 1 and port 2 without using an additional switch. Figure 3.7 illustrates the block diagram of the transceiver's transmitters which were used as RF sources. The digital signal is generated by the Direct Digital Synthesizer (DDS)

that is controlled by software during the measurements. After that it is transmitted by the serial interface JESD204B and after that the signal digitally processed to be converted to analog domain. Once the signal is analog it is filtered, mixed and transmitted.

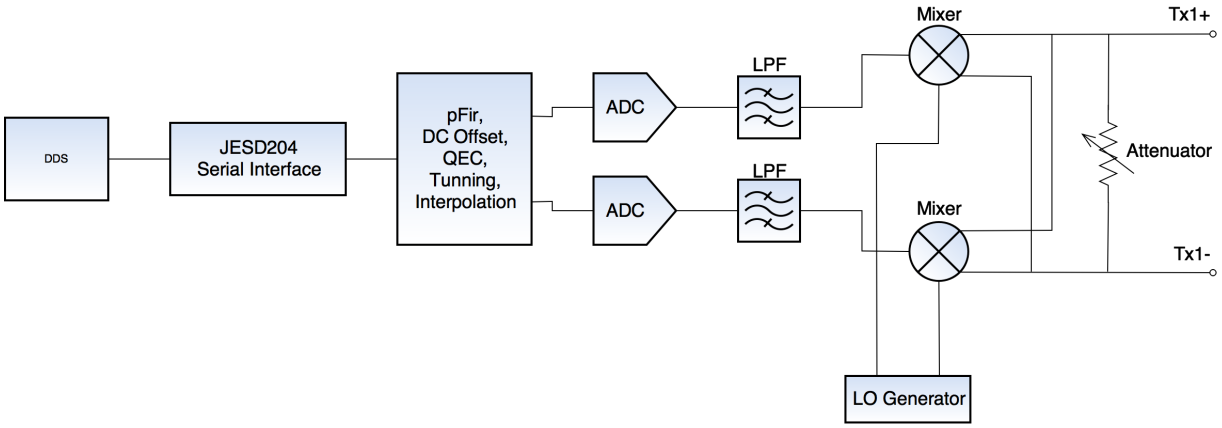

Figure 3.7: Block diagram of the RF transceiver's transmitters used (AD9371)

The next device in the signal path is an RF isolator. The reason for using the isolator is to avoid that the reflected wave reaches the RF source, avoiding this way that the RF source is affected or in the limit be damaged.

The next device in the signal data path is the directional coupler. This allows separate the incident and reflected waves applied to the DUT, waves that will be measured by the RF receivers. Since that the transceiver used only has two receivers and to fully characterize a two-port device it is needed to measure four waves, a switch was necessary. Since it was not possible to get a RF switch that could serve the purpose, the switch is done manually.

The RF receivers used are the same used for the oscilloscope, shown in figure 3.5. After the received waveforms, the waveforms are stored in a FPGA memory and then are sent to MATLAB® through UART, where all processing is performed to calculate the S-parameters and display it in the adequate plots as requested by the user. The user interface used was the MATLAB® GUI.

Figure 3.8 illustrates the setup used for the VNA.

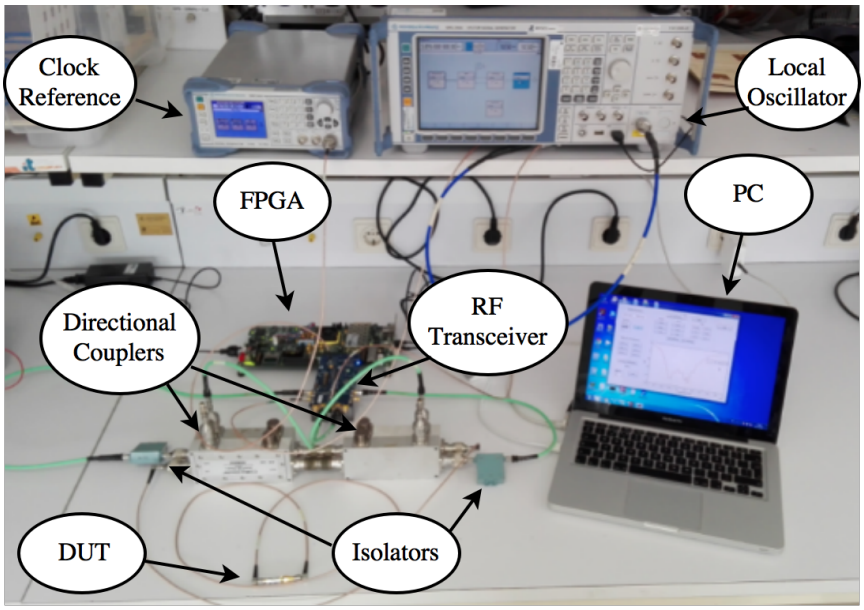

Figure 3.8: Setup of the implemented VNA

Chapter 4

VNA Calibration Procedure Implemented

Prior to measure any device with a VNA it is required to calibrate the VNA in order to eliminate systematic errors. The entire calibration process for one-port and two-port implemented is described on this chapter.

4.1 One-Port Calibration

The one-port calibration starts by calculating the theoretical Γ for each one of the one-port standards at every frequencies that are intended to calibrate. The figure 4.1 illustrates the model, with the signal flow, used to calculate the theoretical reflection coefficient (Γ^M) [19].

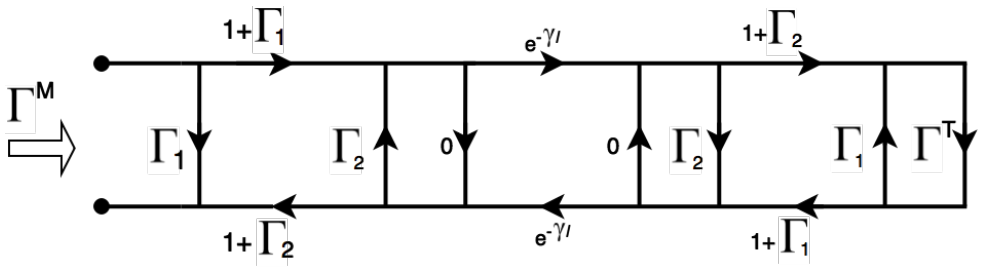

Figure 4.1: Signal flow graph of terminated line model

In figure 4.1:

$$\Gamma_1 = \frac{Z_c - Z_r}{Z_c + Z_r}; \quad \Gamma_2 = -\Gamma_1; \quad \Gamma^T = \frac{Z_T - Z_r}{Z_T + Z_r}; \tag{4.1}$$

$$\gamma = \alpha + j\beta \tag{4.2}$$

where

$Z_c \equiv$ characteristic impedance of line;

$Z_r \equiv$ reference impedance (connector impedance or system impedance)

$\alpha \equiv$ propagation loss constant

$\beta \equiv$ propagation phase constant of line

$l \equiv$ length of line

The characteristic impedance of the line (Z_C) is given by:

$$Z_C = (offset\ Z_0) + (1 - j)(\frac{offset\ loss}{4\pi f})\sqrt{\frac{f}{10^9}} \tag{4.3}$$

The propagation loss constant of the line (α) is given by:

$$\alpha = \frac{(offset\ loss)(offset\ delay)}{2(offset\ z_0)}\sqrt{\frac{f}{10^9}} \tag{4.4}$$

The characteristic impedance of the line (β) is given by:

$$\beta = 2\pi f(offset\ delay) + \alpha \tag{4.5}$$

Where the $offset\ loss$ and $offset\ delay$ are parameters given by the manufacturer of the calibration kit and f is the working frequency.

For Short standard, Γ^T is identified by the subscript S and is calculated as follow:

$$\Gamma_S^T = \frac{Z_s - Z_r}{Z_s + Z_r} \tag{4.6}$$

where

$$Z_s = j2\pi f L_s \quad and \quad L_s = L_0 + L_1 f + L_2 f^2 + L_3 f^3 \tag{4.7}$$

The parameters $L_0, L_1, L_2\ and\ L_3$ are supplied by the manufacturer.

For Open standard Γ^T is identified by the subscript O calculated as by equation 4.8.

$$\Gamma_O^T = \frac{Z_o - Z_r}{Z_o + Z_r} \tag{4.8}$$

where

$$Z_o = j2\pi f C_o \quad and \quad C_o = C_0 + C_1 f + C_2 f^2 + C_3 f^3 \tag{4.9}$$

The parameters C_0, C_1, C_2 *and* C_3 are supplied by the manufacturer.

For Load standard Γ^T is identified by the subscript L calculated as by equation 4.10.

$$\Gamma_L^T = \frac{Z_o - Z_r}{Z_o + Z_r} \tag{4.10}$$

where

$$Z_o = Z_r = 50\Omega \tag{4.11}$$

Now the reflection coefficients of the entire model Γ^Mcan be calculated, applying the calculated parameters of each one of the standards on the equation 4.12. This way the reflection coefficients, Γ_S^M, Γ_O^M and Γ_L^M of the standards Short, Open and Load respectively are calculated.

$$\Gamma^M = \frac{\Gamma_1(1 - e^{-2\gamma l} - \Gamma_1\Gamma^T) + e^{-2\gamma l}\Gamma^T}{1 - \Gamma_1[e^{-2\gamma l}\Gamma_1 + \Gamma^T(1 - e^{-2\gamma l})]} \tag{4.12}$$

After the theoretical Γ is calculated for the three one-port standards, it is needed to calculate the relation between the measured voltage traveling waves (am and bm) and the voltage traveling waves present at the reference plane that are intended to calibrate (ad and bd). The one-port error model and the procedure used to calculate the calibration matrix is based on [20]. The calculated reflection coefficients, Γ_S^M, Γ_O^M and Γ_L^M, are the reflection coefficients for each one of the standards from the calibration plane. The figure 4.2 illustrates two connectors, and its calibration plane [21].

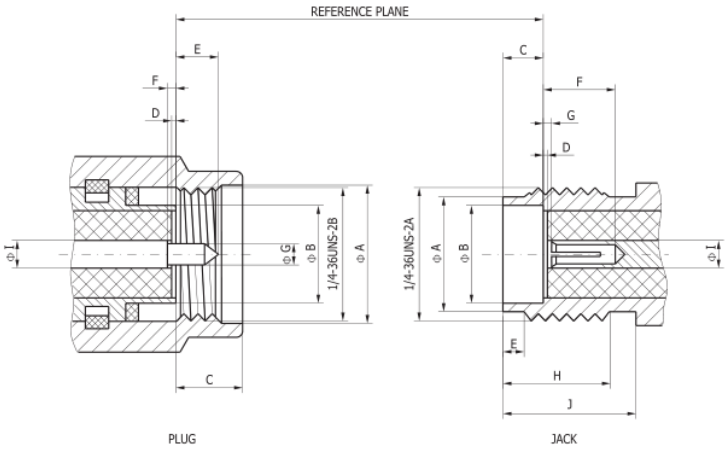

Figure 4.2: Reference plane of two connectors

After calculate the theoretical response of each one of the one-port standards, it is needed to calculate the relation between the measured voltage traveling waveforms and the voltage traveling waveforms present at the calibration plane.

The circuit between the RF receivers and the calibration plane is modeled by figure 4.3.

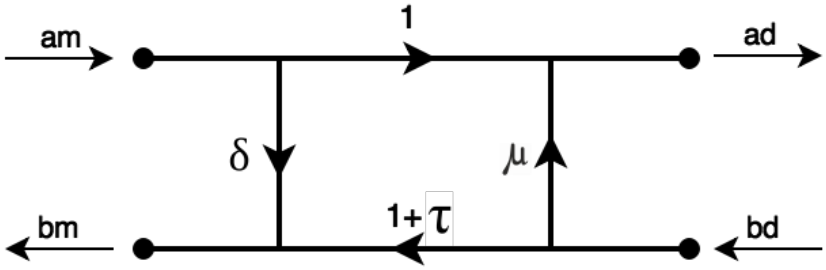

Figure 4.3: One-port error model

In figure 4.3 the residual directivity, δ, is given by :

$$\delta = -(D_1\Gamma_O^M\Gamma_L^M + D_2\Gamma_S^M\Gamma_L^M + D_3\Gamma_S^M\Gamma_O^M) \tag{4.13}$$

The residual source match, μ, is given by:

$$\mu = D_1(\Gamma_O^M + \Gamma_L^M) + D_2(\Gamma_S^M + \Gamma_L^M) + D_3(\Gamma_S^M + \Gamma_O^M) \tag{4.14}$$

The residual reflection tracking, τ, is given by;

$$\tau = -\frac{D_1 + D_2 + D_3}{1 + \tau} \tag{4.15}$$

Where:

$$D_1 = \frac{\Delta\Gamma_S}{(\Gamma_S^M - \Gamma_O^M)(\Gamma_S^M - \Gamma_L^M)}; \tag{4.16}$$

$$D_2 = \frac{\Delta\Gamma_O}{(\Gamma_O^M - \Gamma_L^M)(\Gamma_O^M - \Gamma_S^M)}; \tag{4.17}$$

$$D_3 = \frac{\Delta\Gamma_L}{(\Gamma_L^M - \Gamma_S^M)(\Gamma_L^M - \Gamma_O^M)}; \tag{4.18}$$

where:

$\Delta\Gamma_S \equiv$ error of calibration standard Short

$\Delta\Gamma_O \equiv$ error of calibration standard Open

$\Delta\Gamma_L \equiv$ error of calibration standard Load

Finally it was calculated the relation between the measured voltage traveling waveforms, am and bm, and the voltage traveling waveforms present at the calibration plane, ad and bd.

$$\begin{bmatrix} a_d \\ b_d \end{bmatrix} = \begin{bmatrix} C_{11} & C_{12} \\ C_{21} & C_{22} \end{bmatrix} \begin{bmatrix} a_m \\ b_m \end{bmatrix} \tag{4.19}$$

The parameters C_{11} to C_{22} (matrix C) are deducted from figure 4.3 resulting in equations 4.20.

$$C_{11} = \frac{1+\tau-\mu\delta}{1+\tau}; \quad C_{12} = \frac{\mu}{1+\tau}; \quad C_{21} = \frac{\delta}{1+\tau}; \quad C_{22} = \frac{1}{1+\tau} \tag{4.20}$$

The entire calibration process should be repeated for every frequency points that are intended to calibrate, resulting a C matrix for each frequency point.

4.2 Two-port Calibration

The two-port calibration consists in calibrate each one of the ports separately, according to the process explained in the previous section and then calibrate the "Thru". The "Thru" standard used is the "unknown Thru". The "unknown Thru" is a generic passive reciprocal network. The calibration is achieved by taking advantage of the reciprocal property (S_{12} = S_{21}). After perform the SOL calibration at both ports, one obtains a C matrix, from 4.20 for each port, named $C1$ for port one and $C2$ for port two.

Now it is required to measure the four waves synchronously in two different situations, with signal applied to the port one and port two matched, and the reverse situation, with signal applied to the port two and port one matched. Since the transceiver used only allow to measure synchronously from two RF receivers, instead of measure the four waves at once, a different set of measures was made.

For the situation that the source signal is applied to the port one and the port two is matched the waves at the calibration plane are given by:

$$\begin{bmatrix} a^1_{1,d} \\ b^1_{1,d} \\ a^1_{2,d} \\ b^1_{2,d} \end{bmatrix} = \begin{bmatrix} C1 & 0 \\ 0 & C2 \end{bmatrix} \begin{bmatrix} a^1_{1,m} \\ b^1_{1,m} \\ a^1_{2,m} \\ b^1_{2,m} \end{bmatrix} \tag{4.21}$$

Where the superscript 1 represents the situation where it is applied the exciting signal at the port one and the port two is matched.

Since the waves $a^1_{1,m}$, $b^1_{1,m}$, $a^1_{2,m}$ and $b^1_{2,m}$ can not be measured at once, it was taken three sets os measures to be able to relate all the four waveforms with the same reference. All of the signals measured are referenced to $a^1_{1,m}$, so it is possible to use the four waves ($a^1_{1,m}$, $b^1_{1,m}$, $a^1_{2,m}$ and $b^1_{2,m}$) as if it was measured at once. The receiver one (R_x1) measures the incident waves ($a^1_{1,m}$), and the receiver two (R_x2) measures one of the remaining waveforms at each measure. The numbers inside the circles of figure 4.4 indicate the port measured measured by the receiver two. In other words, it is measured the $a^1_{1,m}$ and $b^1_{2,m}$, then $a^1_{1,m}$ and $a^1_{2,m}$ and lastly $a^1_{1,m}$ and $b^1_{1,m}$, the order of the measures is not important.

The figure 4.4 illustrates how the measures were taken.

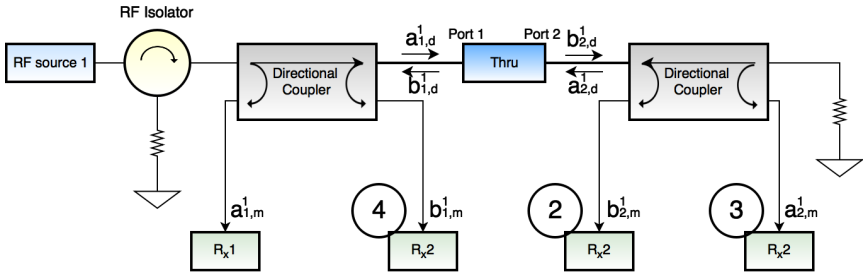

Figure 4.4: Schematic setup for measure the "Thru" with $a_2 = 0$

To reference the measured waves to the same reference used, the phase of the reference waves is subtracted to each one of them as follows:

$$a'^1_{1,m} = \frac{a^1_{1,m}}{e^{j\angle a^1_{1,m}}}; \quad b'^1_{1,m} = \frac{b^1_{1,m}}{e^{j\angle a^1_{1,m}}}; \quad a'^1_{2,m} = \frac{a^1_{2,m}}{e^{j\angle a^1_{1,m}}}; \quad b'^1_{2,m} = \frac{b^1_{2,m}}{e^{j\angle a^1_{1,m}}} \tag{4.22}$$

In 4.22 the angle subtracted to each one of the waves is the angle of measured pair. Now is possible to calculate the waves at the DUT by :

$$\begin{bmatrix} a^1_{1,d} \\ b^1_{1,d} \\ a^1_{2,d} \\ b^1_{2,d} \end{bmatrix} = \begin{bmatrix} C1 & 0 \\ 0 & C2 \end{bmatrix} \begin{bmatrix} a'^1_{1,m} \\ b'^1_{1,m} \\ a'^1_{2,m} \\ b'^1_{2,m} \end{bmatrix} \tag{4.23}$$

For the second situation, the setup used is the one illustrated by figure 4.5

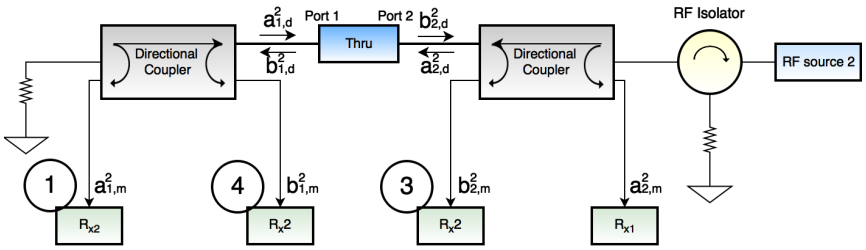

Figure 4.5: Schematic setup for measure the "Thru" with $a_1 = 0$

The measurements are taken in an analogous way to the first situation and this time the reference wave is the $a^2_{2,m}$. The referenced waves are calculated by 4.24.

$$a'^2_{1,m} = \frac{a^2_{1,m}}{e^{j\angle a^2_{2,m}}}; \quad b'^2_{1,m} = \frac{b^2_{1,m}}{e^{j\angle a^2_{2,m}}}; \quad a'^2_{2,m} = \frac{a^2_{2,m}}{e^{j\angle a^2_{2,m}}}; \quad b'^2_{2,m} = \frac{b^2_{2,m}}{e^{j\angle a^2_{2,m}}} \tag{4.24}$$

The waves at the DUT are calculated by:

$$\begin{bmatrix} a^2_{1,d} \\ b^2_{1,d} \\ a^2_{2,d} \\ b^2_{2,d} \end{bmatrix} = \begin{bmatrix} C1 & 0 \\ 0 & C2 \end{bmatrix} \begin{bmatrix} a'^2_{1,m} \\ b'^2_{1,m} \\ a'^2_{2,m} \\ b'^2_{2,m} \end{bmatrix} \tag{4.25}$$

At this point it can be written the following equation:

$$\begin{bmatrix} b^1_{1,d} & b^2_{1,d} \\ b^1_{2,d} & b^2_{2,d} \end{bmatrix} = S_T \begin{bmatrix} a^1_{1,d} & a^2_{1,d} \\ a^1_{2,d} & a^2_{2,d} \end{bmatrix} \tag{4.26}$$

Solving in order to S-parameters (S_T) :

$$S_T = \begin{bmatrix} b^1_{1,d} & b^2_{1,d} \\ b^1_{2,d} & b^2_{2,d} \end{bmatrix} \begin{bmatrix} a^1_{1,d} & a^2_{1,d} \\ a^1_{2,d} & a^2_{2,d} \end{bmatrix}^{-1} \tag{4.27}$$

The "Thru" standard is reciprocal, it has a consistent behaviour , independent of the direction from which it is used. It means that $S_{21} = S_{12}$. To finish the Thru calibration let:

$$S_T = \begin{bmatrix} S_{11} & S'_{12}\alpha \\ S'_{21}\alpha^{-1} & S_{22} \end{bmatrix} \tag{4.28}$$

where :

$$S_{12} = S'_{12}\alpha \quad and \quad S_{21} = S'_{21}\alpha^{-1} \tag{4.29}$$

Taking advantage of the reciprocal property of the "Thru" standard and 4.29:

$$S_{12}\alpha = S_{21}\alpha^{-1} \tag{4.30}$$

So α is given by :

$$\alpha = \pm\sqrt{\frac{S_T(2,1)}{S_T(1,2)}} \tag{4.31}$$

The choose of the sign of α is made based on the electrical length of the "Thru" connection. If the electrical length of the "Thru" standard is smaller than $\lambda/2$ so:

$$\alpha = \sqrt{\frac{S_T(2,1)}{S_T(1,2)}} \tag{4.32}$$

If the electrical length of the "Thru" standard is bigger $\lambda/2$ so:

$$\alpha = -\sqrt{\frac{S_T(2,1)}{S_T(1,2)}} \tag{4.33}$$

The wave length in "Thru" standard is given by:

$$\lambda = \frac{v}{f} \quad and \quad v = \frac{c}{\sqrt{\epsilon_r}} \tag{4.34}$$

where λ is the wavelength, v is the wave propagation speed on the "Thru" standard, f is the working frequency, ϵ_r is the relative permittivity of the dielectric used on the through standard and c is the speed of light in vacuum. The dielectric of the "Thru" standard used is polytetrafluoroethylene that has a $\epsilon_r = 2.1$. The working frequency of the implemented VNA is from 2GHz to 4GHz. So the wave length will be maximum for the minimum working frequency and minimum for the maximum working frequency. Calculating the maximum and minimum wave length of the waves on the "Thru" standard:

$$\lambda_{min} = \frac{3e8/\sqrt{2.1}}{4e9} = 0.052m \quad and \quad \lambda_{max} = \frac{3e8/\sqrt{2.1}}{2e9} = 0.14m. \tag{4.35}$$

The length of the "Thru" standard is equals to 1 cm, so for the entire working frequency of the VNA, α is given by equation 4.32, using this calibration kit. If other calibration kit

is used, the calibration kit parameters must be updated. The resultant calibration matrix for two-port case is the following one:

$$C_T = \begin{bmatrix} C_1 & 0 \\ 0 & \alpha C_2 \end{bmatrix} \tag{4.36}$$

The calibration process is finished with the calculation of C_T. Similarly to one-port calibration the two-port calibration process is performed for every points in frequency that is intended to calculate the S-parameters.

Chapter 5

Practical Results

5.1 Power Meter

The power detector used is able to measure RMS power over a frequency range of 40 MHz to 6GHz, but for frequencies above 3 GHz a differential input matching is required to improve the isolation. Since the input matching was not implemented, the power meter was tested only up to 3 GHz.

To test and evaluate the power meter it was measured the power of signals which power is known along the entire power range of the implemented power meter (-56 dBm to 2 dBm). This process was repeated with signals at different frequencies covering this way the frequency range of 40 MHz to 3 GHz.

Figure 5.1 illustrates the power values of a signal at 50 MHz, 1 GHz and 3 GHz measured by the implemented power meter.

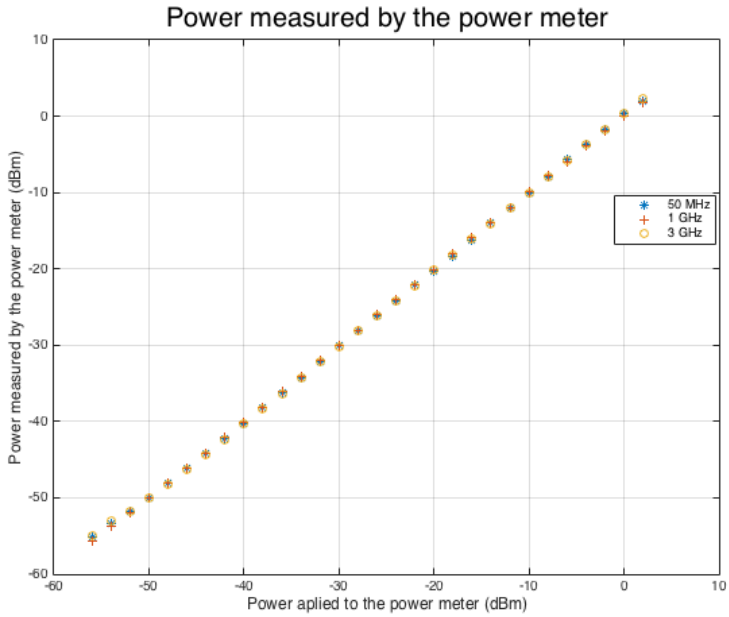

Figure 5.1: Power measured by the implemented power meter of signals at 50 MHz, 1 GHz and 3 GHz

Figure 5.2 illustrates the errors of the power measured by the power meter.

Figure 5.2: Errors of power measured by the implemented power meter of signals at 50MHz, 1 GHz and 3GHz

By the errors presented by the figure 5.2 is visible that the maximum error is of 1.1 dB for 3 GHz when the input signal is -56 dBm. The variance of the measured power is

higher close to the limits of the frequency and power ranges, as expected since outside of the frequency range or power range the values behaviour of the power detector became not linear with the input power.

5.2 Oscilloscope

The implemented oscilloscope has different characteristics from the traditional ones. Since the receivers of the oscilloscope are based on a homodyne architecture, figure 3.5, the signal is sampled in baseband. So, it is only possible to visualize the slower spectral components around the LO frequency. The oscilloscope displays the input signal around the central frequency settled by the user, with 100MHz bandwidth (ADCs' bandwidth) with a sampling frequency of 122.88MHz. This makes the implemented oscilloscope different from the commercial ones, that sample and display the signals at their absolute frequency.

The following subsections describe the implemented oscilloscope.

5.2.1 Finite State Machine

The control system of the oscilloscope, illustrated by figure 5.3, is handled by two FSM: one on the MATLAB® side which works as master and another one on the FPGA side which works as slave. The FSM from the MATLAB® side has three states and one input signal. The "Initial" state decides if the next state is "Receive" or "Configure", based on the value of the input signal "New Conf" and sends a three-characters word to the FPGA indicating the next state. The input signal "New Conf" indicates if the configurations were updated by the user or not. The "Receive" state just receives the waveforms from FPGA and the "Configure" state sends the updated configurations to FPGA. The following state of both "Receive" and "Configure" states is always the "Initial" state. On the FPGA side the program waits for the reception of three characters that carry the information about what to do next. If the information carried by the characters indicates to configure, the program waits for the reception of the set of configurations and the transceiver configurations are updated. If the information carried by the characters indicates to send data, an actualized waveform is sent to MATLAB®.

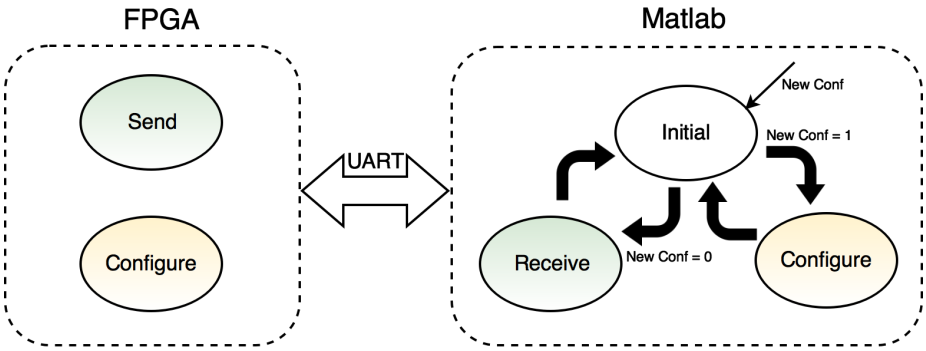

Figure 5.3: FSM responsible for controlling the oscilloscope

5.2.2 Interface

The oscilloscope interface is presented in figure 5.4. The entire interaction between the oscilloscope and the user is performed through this interface. It allows to control the central frequency of the oscilloscope, the trigger systems, the vertical and horizontal systems, and chose what channel to visualize. The available controls will be explained as it follows.

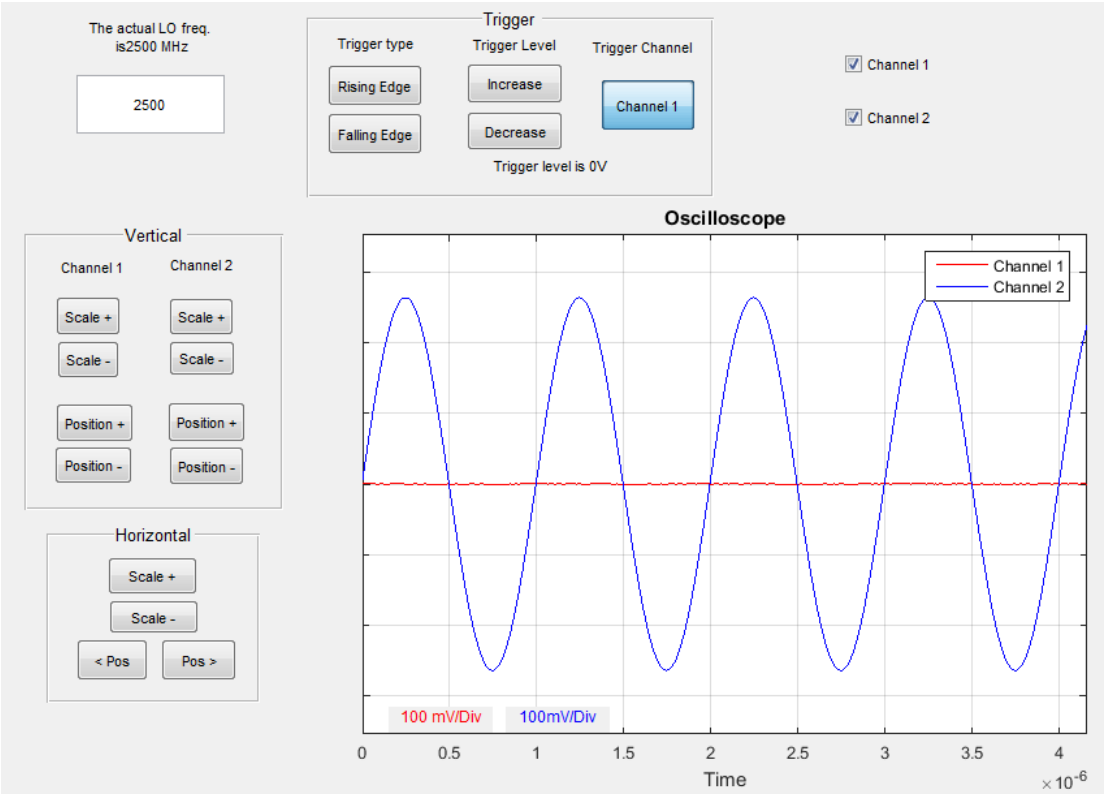

Figure 5.4: Oscilloscope interface

LO Frequency

The LO frequency is one of the parameters that the user can define in this oscilloscope. When the oscilloscope is turned on, the LO frequency is settled to a default frequency, which is displayed in the upper left corner of the oscilloscope window (figure 5.4). In the box below, it is possible to change the LO frequency within a range of 400MHz to 6GHz. When the user changes the LO frequency the FSM enters the "Configure" state and sends the updated set of configuration parameters to the FPGA. In FPGA the frequency of the LO is settled to the desired value. The LO is generated by the clock generator AD9528, which is integrated in the RF transceiver.

Vertical System

The vertical system is totally implemented in MATLAB®. The hardware used does not allow the same flexibility that the hardware of a commercial oscilloscopes does, so some functions that are usually implemented in hardware were implemented in software. These differences offer higher simplicity in the implementation, at the cost of getting lower performances.

The implemented vertical system allows to change the position and scale of each channel. The information about scale and vertical position of each channel is stored in MATLAB® variables, so the waveforms can be scaled and positioned according to what the user defined. The transceiver's ADCs, that are responsible for the sampling are 16 bits, and their full-scale voltage is of 0.707 mV.

Horizontal System

The horizontal system is also controlled in MATLAB®, with a similar process to the vertical system. The information about the horizontal scale and position is also stored in MATLAB® variables and the received waveform is scaled and positioned accordingly to that information.

Acquisition system

The acquisition system is not evidenced in the user interface, but it is possible to change some parameters by software. The record length is flexible, it can be any power of two below 32384 samples, to not exceed the memory available, in both MATLAB® and FPGA side. The MATLAB® and FPGA communicate by UART, which can get slower for transferring big sizes of data even working at the maximum baudrate allowed by the

system (921.6 kbps). Hence, the waveform update rate of the oscilloscope is limited by the waveform transfer rate of the UART and when the record length increases, the waveform transfer time increases in the same proportion. With the record length of 1024 sampled points and two channels, the waveform update rate is approximately of 4 wfms/s.

Trigger System

Due to limitations on hardware the trigger systems could not be implemented as in commercial oscilloscopes. Instead of having a system to determine when the ADC should start sampling, the sampling starts as soon as the system is available and the trigger is performed by software. The user can choose the trigger type, adjust the trigger level and choose the trigger channel on the panel of the oscilloscope interface. The trigger information is saved in a MATLAB® variable and when the waveforms are received it is processed to find the first point that accomplishes the trigger conditions. The waveforms are displayed from that point, dropping the unwanted samples. By performing the trigger like this, it is inevitable to lose sampled data. The trigger max deviation corresponds to the ADC sample time that is $\frac{1}{ADC\ Sample\ rate} = \frac{1}{122.88MHz} = 8.14\eta s$.

Channel selection

The oscilloscope has two available channels and the user can select the one desired to analyze or both in the upper right corner of the interface. The number of channels selected influences the waveform update rate, because the UART only transfers the data related to the channels selected. Hence, with only one channel selected the waveform update rate will be roughly twice as it would be with two channels.

5.2.3 Results

To evaluate the veracity of the data acquired by the implemented oscilloscope an waveform acquired by the implemented oscilloscope is compared with the same waveform measured by a commercial sampling oscilloscope. The signal measured is a two tone signal with one tone at 990 MHz and the other one at 1010 MHz. The signal measured by the implemented oscilloscope is down-converted with the LO at 1 GHz, resulting a baseband at 10 MHz. The signal measured by the sampling oscilloscope is sampled from RF. Figure 5.5 illustrates the waveform acquired by the implemented oscilloscope and by the commercial sampling oscilloscope.

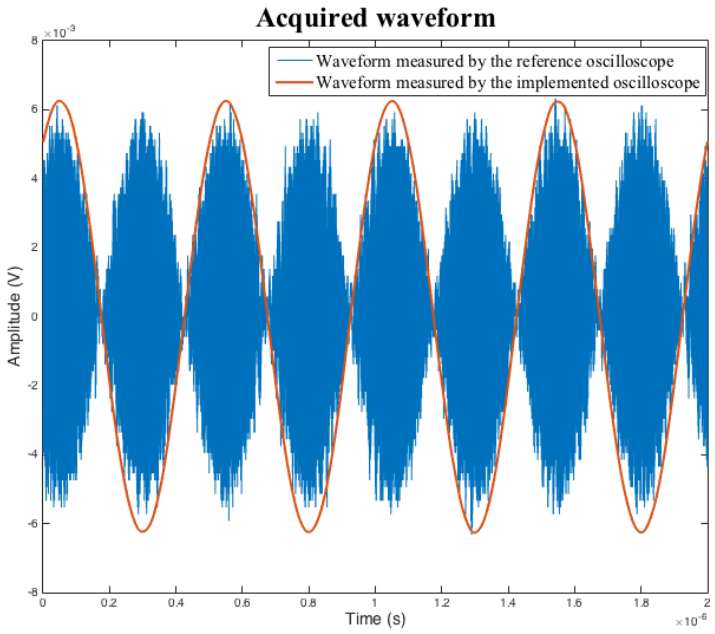

Figure 5.5: Waveform acquired by the implemented oscilloscope and acquired by a reference sampling oscilloscope

By figure 5.5 it is visible that the waveform acquired by the implemented oscilloscope corresponds to the envelope of the waveform acquired by the commercial sampling oscilloscope, as expected. The resolution of the commercial sampling oscilloscope is 100 ps and the ADC sampling rate of the implemented oscilloscope is 122.88 MHz, hence it's resolution is 8.138 ηs.

5.3 VNA

The practical results of the implemented VNA are presented on this section. First the FSM implemented is explained, then the user interface is presented. After that the results of the measures performed are presented.

5.3.1 Finite State Machine

Similarly to the oscilloscope, the VNA is controlled by a FSM, illustrated by figure 5.6. The FSM principle is the same as the one implemented for the oscilloscope, but in this case it has one more state. The "Initial" and "Receive" states have the same functions that the the ones in the oscilloscope FSM. The new state ("Send") is required to send to FPGA the

frequency at which the RF source should transmit the signal. From MATLAB® side, the FSM is started at "Initial" state, then if the the configurations were updated (New Conf =1), the next state is "Configure"; if not, the next state is "Send". After the "Send" and "Configure " states the FSM always returns to the "Initial" state. When the FSM returns to the "Initial" state from the "Send", the next state is "Receive" and from "Receive" it always return to the "Initial" state. This process is repeated for every frequency point intended to be measured.

From the FPGA side the action is controlled by the commands sent from MATLAB®, as in the oscilloscope. In this case, the FPGA also receive the frequency at which the RF transmitters should transmit from MATLAB® to configure the DDS.

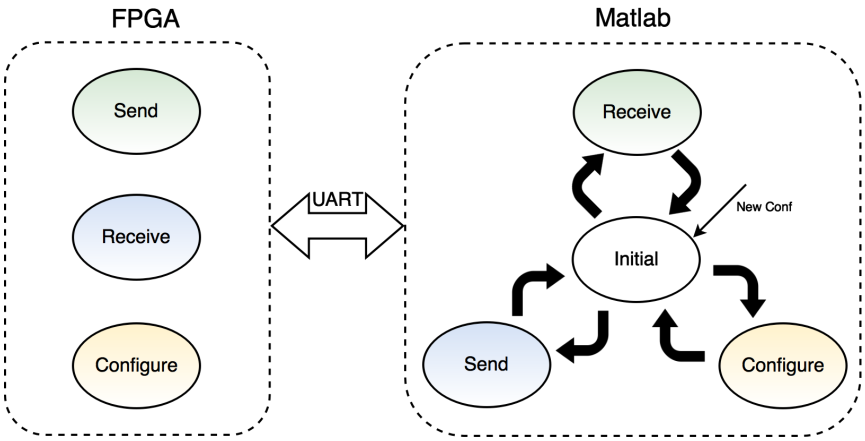

Figure 5.6: FSM implemented for VNA

5.3.2 Interface

The interface implemented for the VNA is the one presented by figure 5.7. It allows the user to define the frequency sweep intended, the type of calibration (one or two port) and, after being calculated, it allows to visualize the measured S-parameters by rectangular graph or Smith chart.

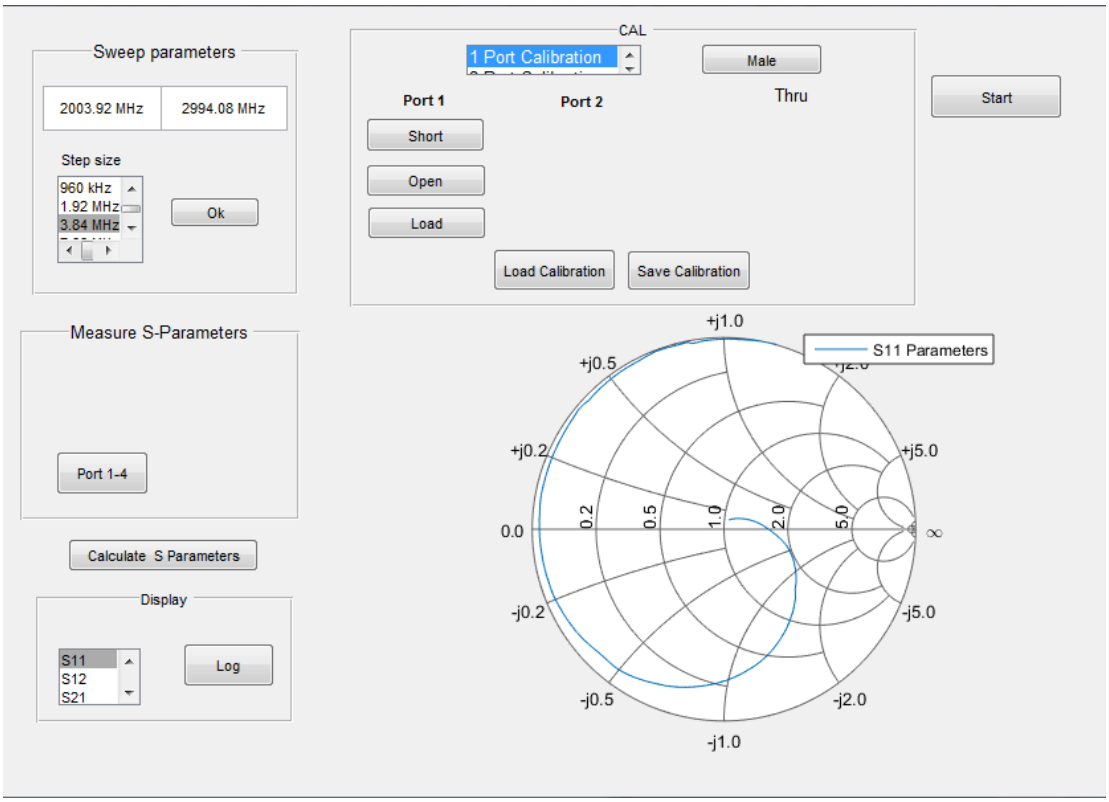

Figure 5.7: VNA's user Interface with one-port calibration selected and the S_{11} parameters displayed in a smith-chart

Sweep Parameters

Before calibration, the user should define the sweep parameters. The sweep parameters which should be defined are the start frequency, stop frequency and the step size. After defining the parameters and clicking "ok", the frequency sweep is calculated. If the sweep defined by the user is smaller than the ADCs bandwidth, the LO frequency is settled to the center of the defined sweep. After that a vector is calculated with frequency values from $-\frac{BB\_sweep}{2}$ to $\frac{BB\_sweep}{2}$ with spacing equal to the step defined by the user. BB_sweep is the frequency sweep size that is performed, only changing the frequency of the baseband signal. If the sweep is larger than the bandwidth of ADCs, it is divided in smaller intervals and the LO frequency is shifted for each one, and the sweep is calculated as described in the previous case. The sweep calculation is illustrated by figure 5.8.

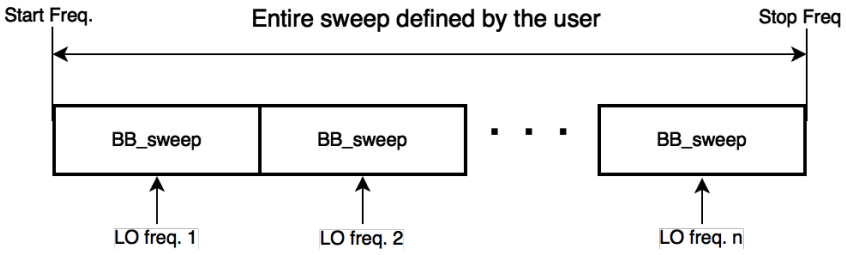

Figure 5.8: Sweep calculation schematic

Calibration

The calibration panel "CAL" of the VNA user interface allows the user to perform the calibration. The user should start by choosing the calibration type, after that he can load a calibration previously saved or perform the calibration. When the user is calibrating the VNA, depending on the type of calibration selected, one-port or two-port, the calibration procedure is different, as explained in Chapter 4. In the "CAL" panel the user has a button for each measurement required. Before pressing the button, the user should correctly connect the RF receivers and the standards as described in Chapter 4. Figure 5.7 illustrates the interface when the one-port calibration is selected, and figure 5.9 illustrates the interface when the two-port calibration is selected. When the user selects, for example, "Short", firstly the FSM goes to the "Configure" state to set the first LO frequency, then each frequency of the *B_sweep* is sent to FPGA and lastly the desired waves are measured by the RF receivers and sent to MATLAB®. The MATLAB® receives the measured waves and saves the relevant spectral information.

After the calibration is done, it can be saved using the button on the panel, in a .mat file.

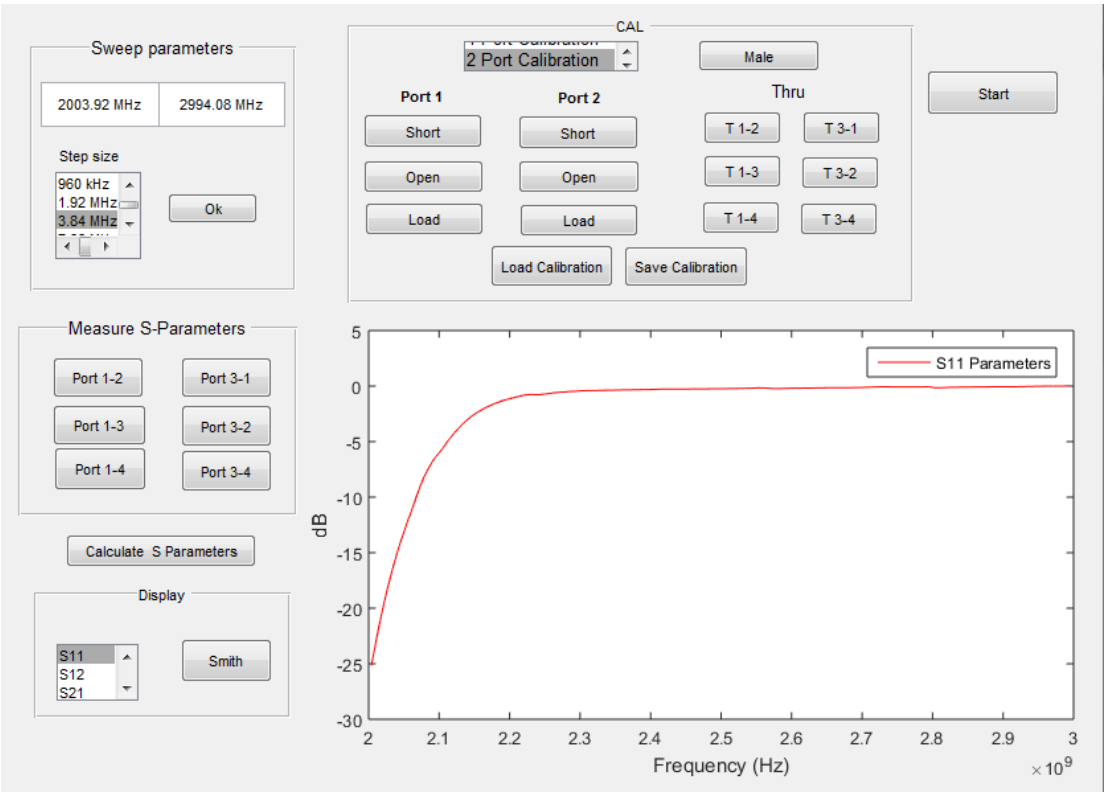

Figure 5.9: VNA Interface with two-port calibration selected and the S_{11} parameters displayed in a logarithmic graph

Measuring the Device

After calibration, the DUT can be measured to calculate the S-parameters. In the case of a one-port DUT, only the incident and reflected waves are necessary to be measured. It is done by clicking on button "Port1-4" button of the interface, figure 5.7. The process for measuring is exactly the same described for one of the one-port calibration standards, but in this case with the DUT connected instead of the standard.

In the case of a two-port DUT the process is similar to the process used for the "Thru" calibration. This time, instead of connecting the "Thru", the DUT is connected and the panel used in the user interface is the "Measure S-Parameters".

After finishing all the measurements, the user can calculate the S-parameters by clicking on the "Calculate S Parameters" button. If a loaded calibration is used, the S-parameters are directly calculated using the loaded calibration matrices. If a calibration was measured, the calibration matrices are calculated and then the S-parameters are calculated.

Display

When all the measurements are finished, the user can visualize the S-parameters in two different formats. In the "Display" panel the parameter to visualize can be selected as well as the format. Logarithmic graph or smith-chart that are the most common formats to visualize the S-parameters. In figure 5.7 it is illustrated the VNA interface displaying the S_{11} parameters in a smith-chart.

5.3.3 Measured standards

One of the measurements that can be made to verify the veracity of the calibration process implemented is the measurement of the one-port standards. The one-port standards were measured using the implemented VNA and a reference VNA. The calibration kit used to calibrate the reference VNA was not the same that was used to calibrate the implemented VNA. On one hand, different calibration kits were used because the calibration kit used in the reference VNA is commonly used in the RF lab, so it was not possible to use it for all the tests. On the other hand, the kit used on the implemented VNA did not have the correct model on the reference VNA. Since different calibration kits were used, it was not possible to identify the errors introduced by the calibration model and the errors introduced by the measurement. Despite that, it is still useful to compare the response of the standards measured by the reference VNA with the theoretical response of the standards because it is an indication that the model used is valid.

All S-parameters measurements presented in this dissertation were performed from 2 GHz to 3 GHz with a frequency step of 3.84 MHz. It is difficult to obtain a frequency sweep calculated by the implemented VNA equal to the one calculated by the reference VNA. This is due to the fact that the reference VNA allows to set the number of frequency points and the implemented VNA allows to set the frequency step. Beyond that, the RF transceiver used only allows to set the LO in a predefined grid of frequencies what forces small adjustments on the sweep defined by the user. So, to evaluate the errors between the two measurements a cubic interpolation was made to get the parameters on the same frequency points.

Short

Figure 5.10 illustrates the S_{11} parameters of the short standard, calculated by the theoretical model and the S_{11} parameters of the short standard measured by the reference VNA. It is possible to verify by figure 5.10 that the short standard is not an ideal short,

as expected. Both responses have very close phases that are rotating clockwise like the phase of any physical device. A difference in magnitude between the two measurements is visible: the S_{11} parameters measured by the reference VNA present smaller magnitude value than the theoretical S_{11} parameters. The reason for this difference can be losses not considered in the model.

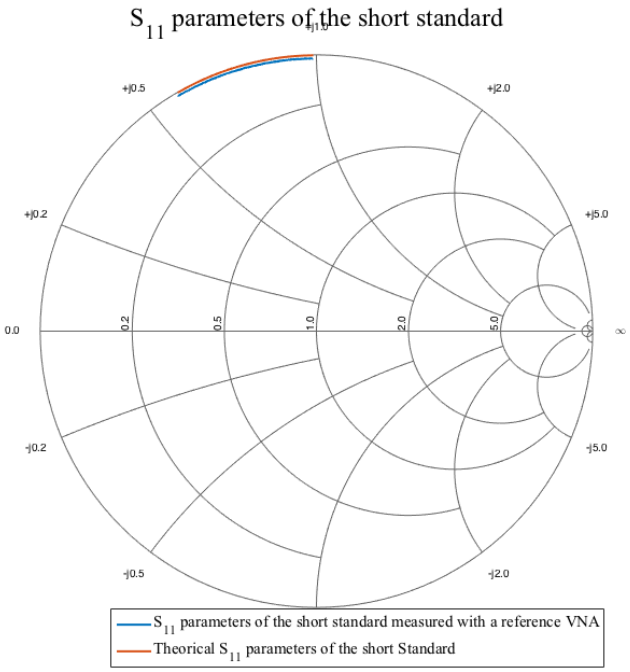

Figure 5.10: S_{11} parameters of the short standard:
theoretical vs measured by the reference VNA

Figure 5.11 illustrates the magnitude and phase errors between the theoretical response of the short standard and the response measured by the reference VNA. The maximum absolute error is -37dB and the maximum phase error is of 0.5 degrees.

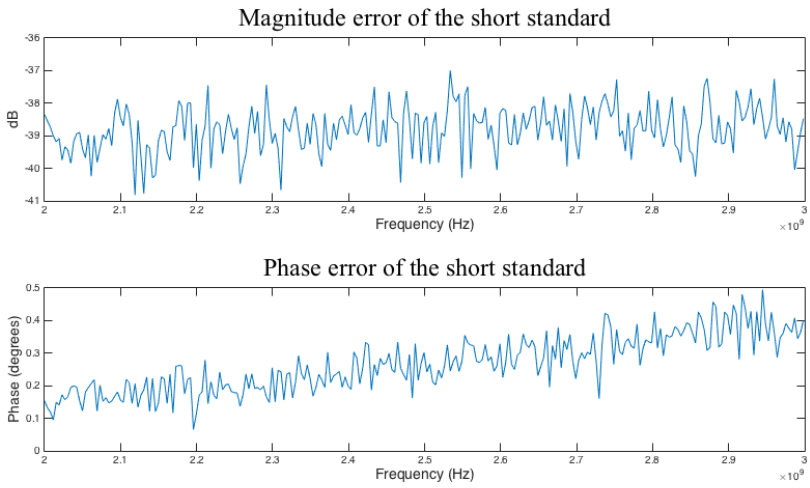

Figure 5.11: Magnitude and phase errors of the short S_{11} parameters: errors between theoretical S_{11} parameters and S_{11} parameters measured by the reference VNA

Figure 5.12 illustrates the theoretical S_{11} parameters of the short standards and the S_{11} parameters measured by the implemented VNA of the short standard.

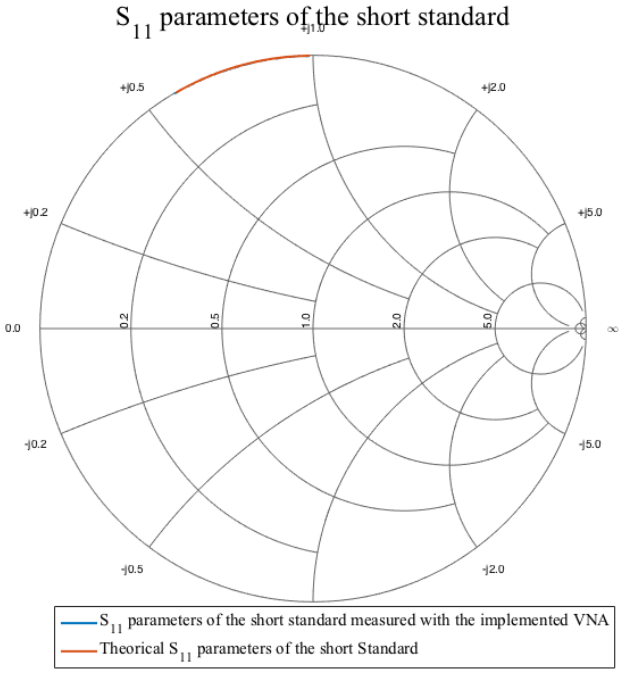

Figure 5.12: S_{11} parameters of the short standard: theoretical vs measured by the implemented VNA

Figure 5.13 illustrates the magnitude and phase errors between the theoretical S_{11} parameters of the short standard and the S_{11} parameters of the short standard measured by the implemented VNA. The maximum magnitude error is -45dB and the maximum phase error is 0.55 degrees.

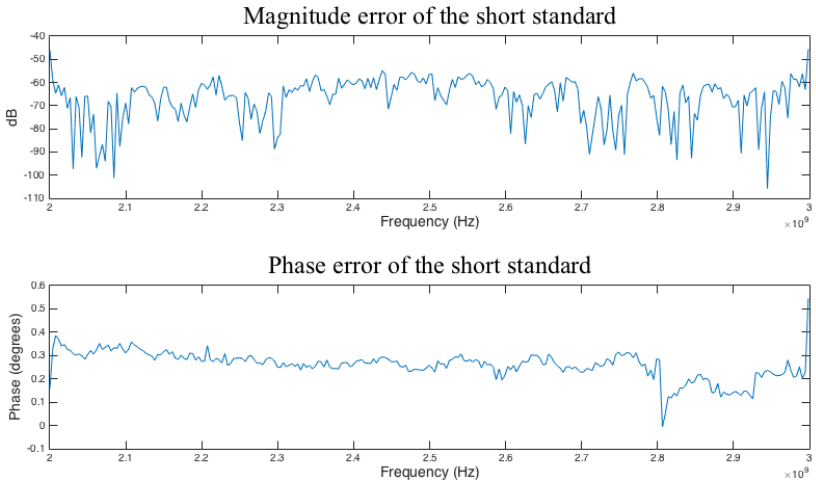

Figure 5.13: Magnitude and phase errors of the short S_{11} parameters: errors between theoretical S_{11} parameters and S_{11} parameters measured by the implemented VNA

Open

The second standard measured was the open standard. In figure 5.14 the theoretical S_{11} parameters of the open standard and the S_{11} parameters of the open standard measured by the reference VNA are illustrated.

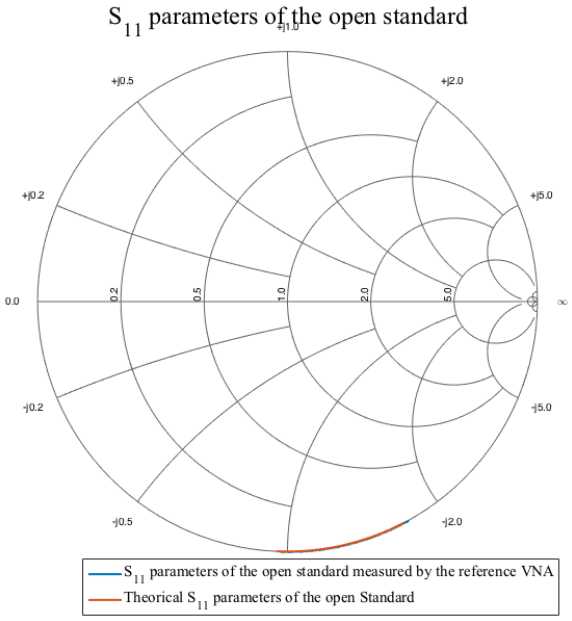

Figure 5.14: S_{11} parameters of the open standard:
theoretical vs measured by the reference VNA

In figure 5.15 the magnitude and phase errors between the theoretical S_{11} parameters and the S_{11} parameters of the open standard measured by the reference VNA are illustrated. The maximum magnitude error is -45dB, and the maximum phase error is 1.25 degrees.

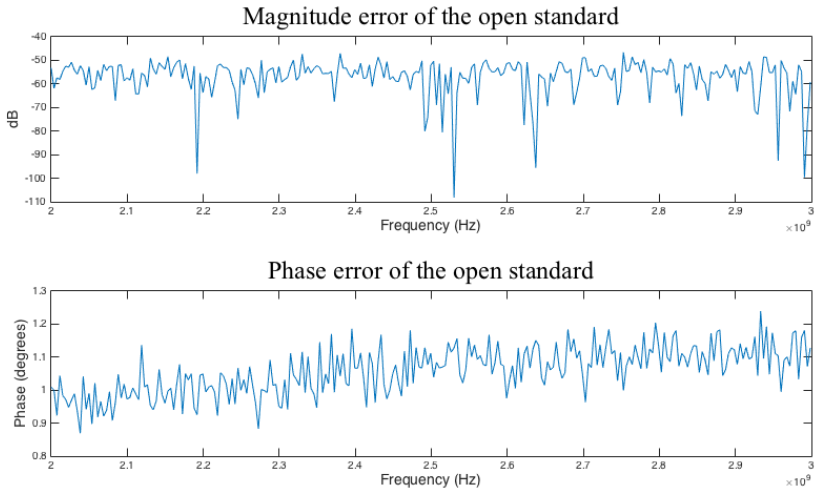

Figure 5.15: Magnitude and phase errors of the open S_{11} parameters:
errors between theoretical S_{11} parameters and S_{11} parameters measured by the reference VNA

Figure 5.16 illustrates the theoretical S_{11} parameters and the S_{11} parameters of the open standard measured by the implemented VNA.

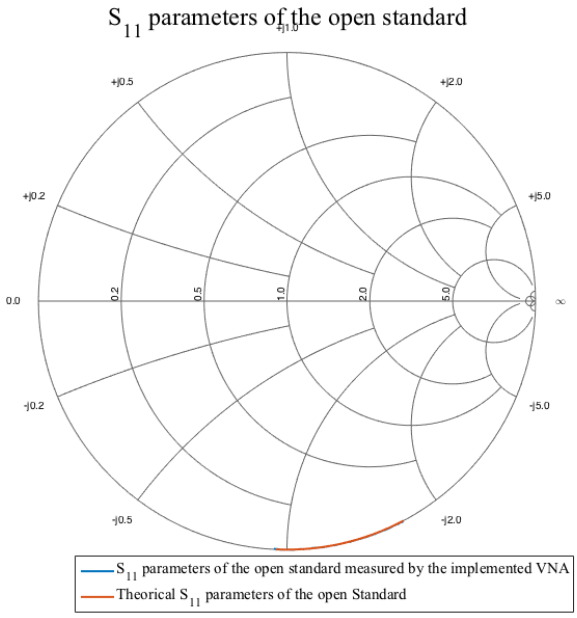

Figure 5.16: S_{11} parameters of the open standard:
theoretical vs measured by the implemented VNA

In figure 5.17 the magnitude and phase errors between the theoretical S_{11} parameters and the S_{11} parameters of the open standard measured by the implemented VNA are illustrated. The maximum magnitude error is -52dB, and the maximum phase error is of 0.45 degrees.

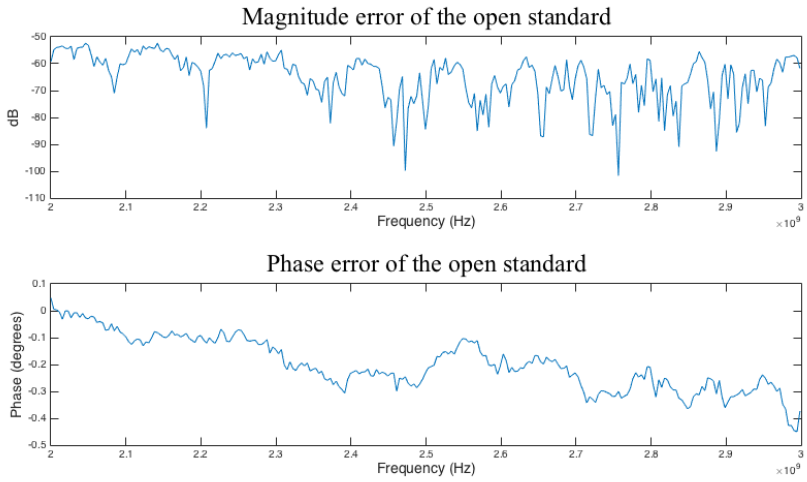

Figure 5.17: Magnitude and phase errors of the open S_{11} parameters: errors between theoretical S_{11} parameters and S_{11} parameters measured by the implemented VNA

Load

The last one-port standard to be measured was the Load standard. In figure 5.18 the theoretical S_{11} parameters and the S_{11} parameters of the load standard are illustrated.

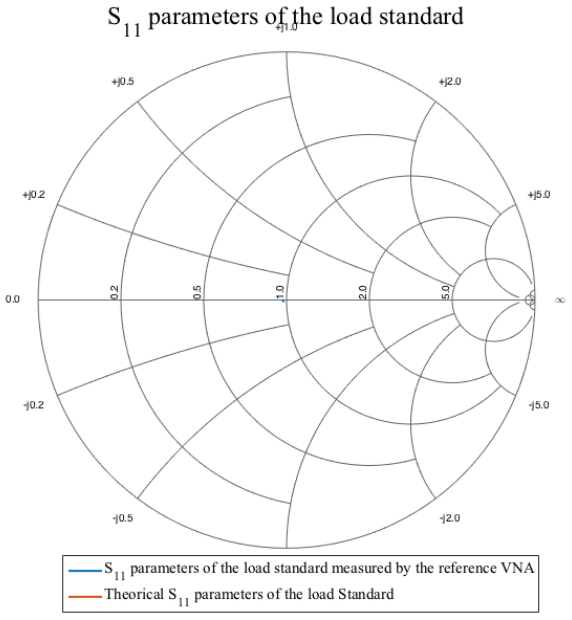

Figure 5.18: S_{11} parameters of the load standard: theoretical vs measured by the reference VNA

In figure 5.19 the magnitude and phase errors between the theoretical S_{11} parameters and the S_{11} parameters measured by the reference VNA of the load standard are illustrated. The maximum magnitude error is of -35.9dB, and the maximum phase error is of 178 degrees.

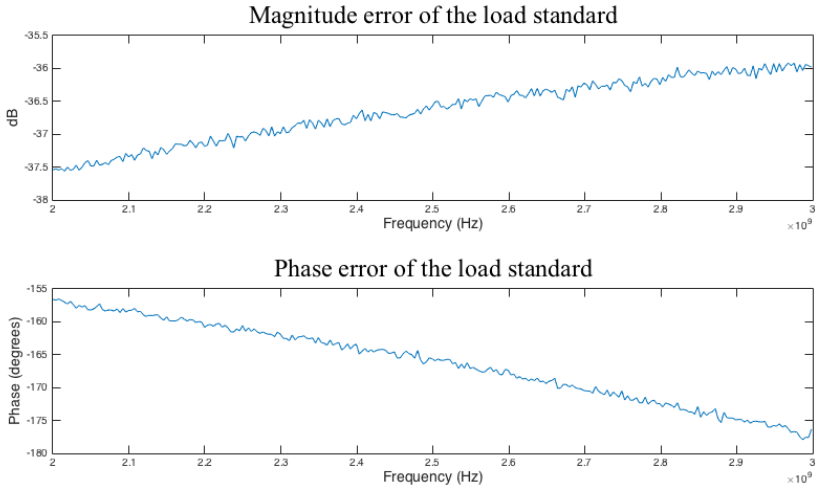

Figure 5.19: Magnitude and phase errors of the load S_{11} parameters:
errors between theoretical S_{11} parameters and S_{11} parameters measured by the reference VNA

Figure 5.20 illustrates the theoretical S_{11} parameters and the S_{11} parameters measured by the implemented VNA of the load standard.

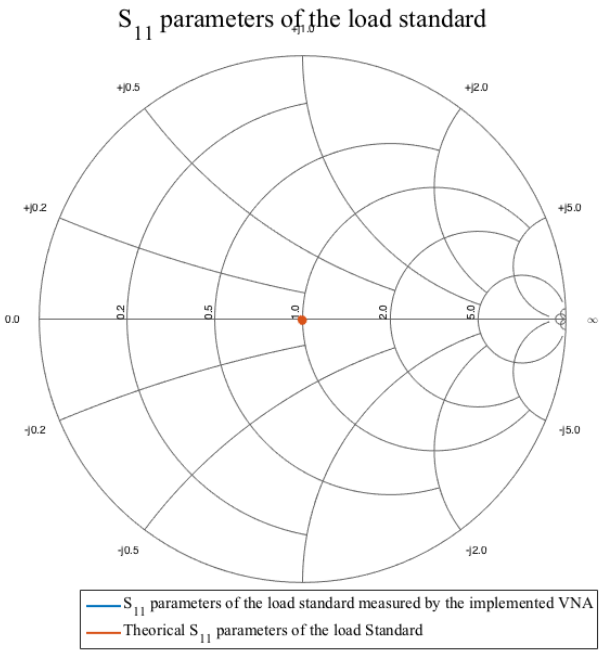

Figure 5.20: S_{11} parameters of the load standard: theoretical vs measured by the implemented VNA

In figure 5.21 the magnitude and phase errors between the theoretical S_{11} parameters and the S_{11} parameters measured by the implemented VNA of the load standard are illustrated. The maximum magnitude error is of -35dB. In both figures 5.21 and 5.19 the phase error is due to the fact that the theoretical model considers an ideal load. In this case the phase error is not relevant because the imaginary part of the S_{11} parameters measured is very close to zero.

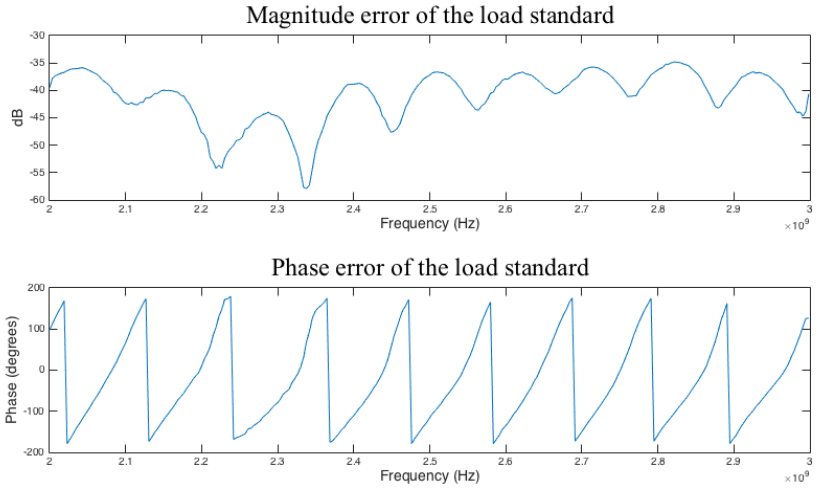

Figure 5.21: Magnitude and phase errors of the load S_{11} parameters: errors between theoretical S_{11} parameters and S_{11} parameters measured by the implemented VNA

The magnitude error between the theoretical S_{11} parameters of the standards and the S_{11} parameters measured by the reference VNA is lower than -37dB for the three calibration standards. The phase error also between the theoretical S_{11} parameters and the S_{11} parameters measured by the reference VNA is lower than 1.25 degrees for short and open standards. The phase error of the load standard is not meaningful as explained above. These results show that the model used for the calibration standards is valid, since the errors presented are suitable for the goals of this project.

Now, analyzing the errors between the theoretical S_{11} parameters of the standards and the S_{11} parameters measured by the implemented VNA. The magnitude error is lower than -35dB for the three calibration standards and the phase error is lower than 0.55 degrees for short and open standards. The phase error of the load standard is not meaningful as explained above. These results demonstrate that the measurements taken by the implemented VNA have good repeatability. Repeatability is very important in a VNA because even if an error is introduced in the measurements, the resulting S-parameters can be corrected if this error is constant, because the calibration process will eliminate it.

5.3.4 First Device Measured

After the calibration process is validated, a few devices were measured by the implemented VNA. The first one-port device measured was a filter terminated by a load at one

of the ports. The filter used was a low-pass filter with a cut frequency of 2GHz. A filter as one-port device was used because it was available in the laboratory and the measurements of a filter are stable. The S_{11} parameters of the filter measured by the implemented VNA are compared with the S_{11} parameters measured by the reference VNA. In figure 5.22 both S_{11} parameters measured by the implemented VNA and measured by the reference VNA are illustrated.

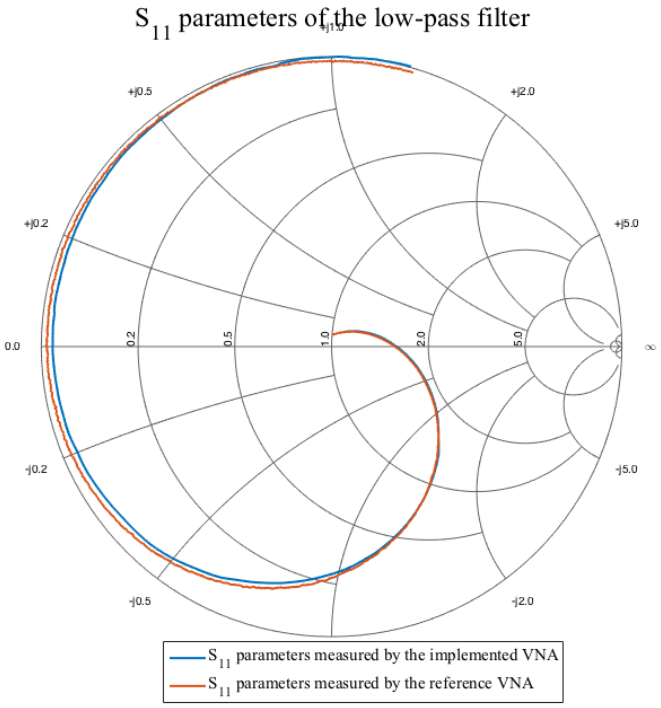

Figure 5.22: S_{11} parameters of the low-pass filter:
measured by the reference VNA vs measured by the implemented VNA

Figure 5.23 illustrates the magnitude and phase errors between the S_{11} parameters measured by the implemented VNA and the S_{11} parameters measured by the reference VNA. The maximum magnitude error is of -35dB and the maximum phase error is of 15 degrees.

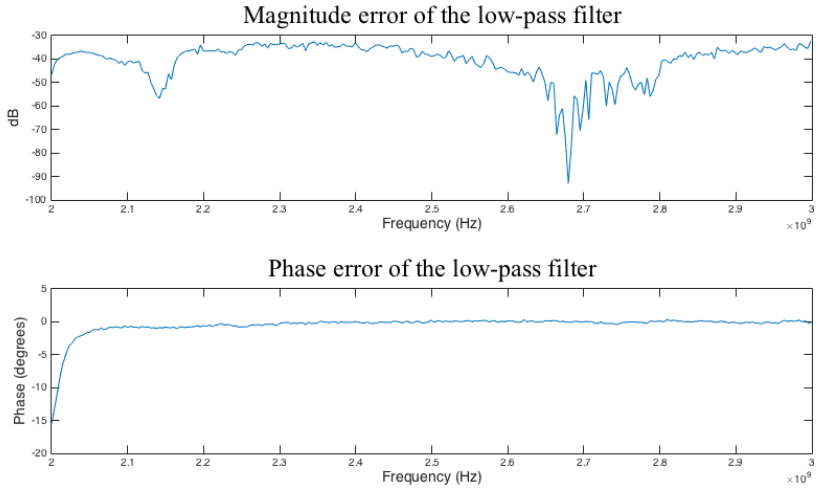

Figure 5.23: Magnitude and phase errors of the S_{11} parameters:
errors between S_{11} parameters measured by the reference VNA and S_{11} parameters measured by the implemented VNA

The measurements of one-port devices are satisfactory. The resulting S-parameters present the behaviour expected and the errors associated to the measurement when compared to the same measure performed by a reference VNA are acceptable. The magnitude error is always lower than -35dB, which is an acceptable value. The phase error has a maximum at 2 GHz of 15 degrees but on the rest of the band is much lower, which means that at this specific frequency there is an unknown measuring error. And the impedance is close to the center where a large phase error is not very significant since the impedance is dominated by the real part and a small error on the imaginary impedance causes a large phase variations.

5.3.5 Second Device Measured

The second device measured was a band-pass filter with passing band between 2340 MHz and 2530 MHz. The four S-parameters of this filter were measured by the implemented VNA and compared with the same S-parameters measured by the reference VNA. In figure 5.24 the S_{11} parameters of the filter are represented, measured by the implemented VNA and by the reference VNA.

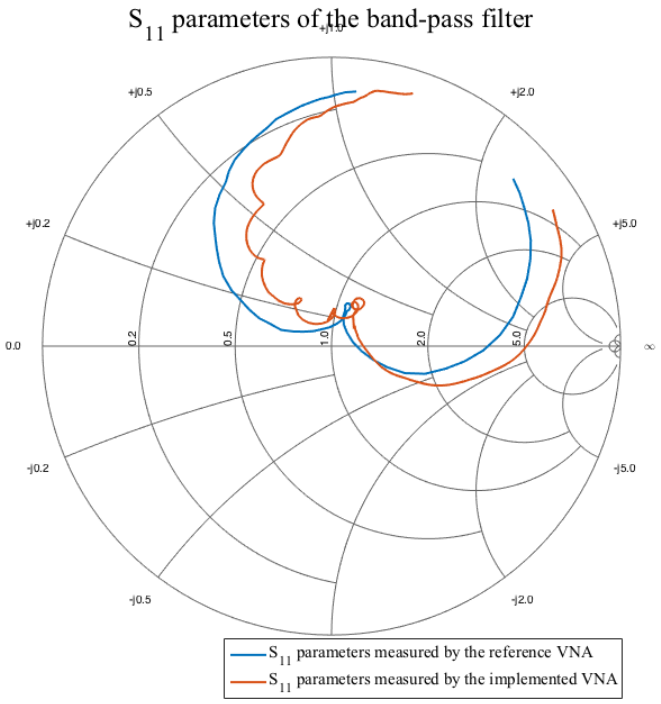

Figure 5.24: S_{11} parameters of the band-pass filter:
measured by the reference VNA vs measured by the implemented VNA

Figure 5.25 illustrates the magnitude and phase errors between the S_{11} parameters of the filter measured by the reference VNA and the S_{11} parameters of the filter measured by the implemented VNA. The magnitude maximum error is of -23dB and the maximum phase error is of 40 degrees.

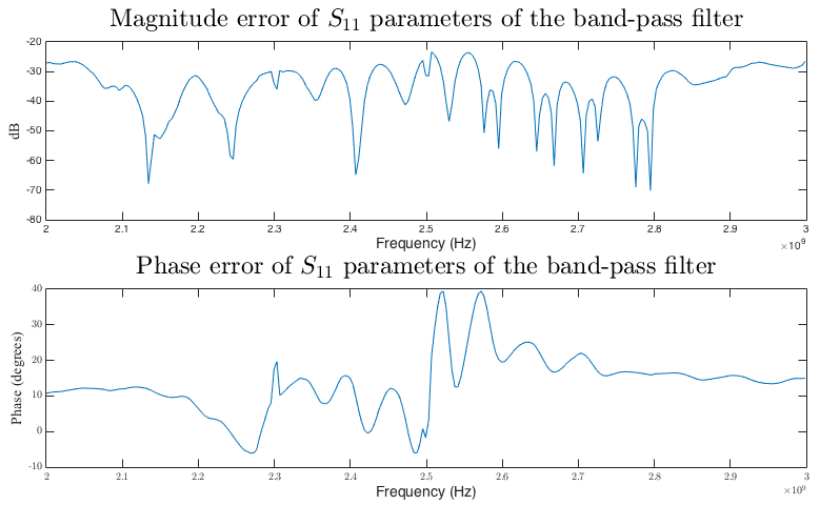

Figure 5.25: Magnitude and phase errors of the S_{11} parameters:
errors between S_{11} parameters measured by the reference VNA and S_{11} parameters measured by the implemented VNA

Figure 5.26 illustrates the S_{22} parameters of the filter measured by the implemented VNA and the S_{22} parameters of the filter measured by the reference VNA.

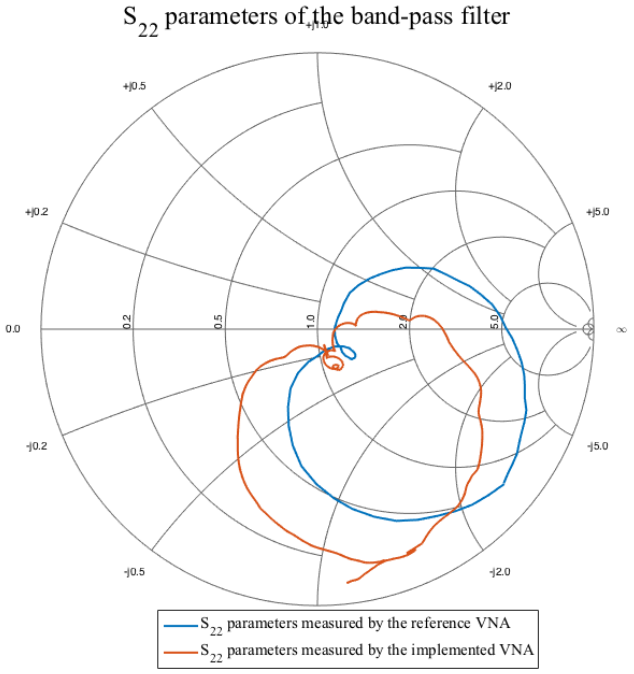

Figure 5.26: S_{22} parameters of the band-pass filter:
measured by the reference VNA vs measured by the implemented VNA

The errors between the S_{22} parameters measured by the reference VNA and the S_{22} parameters measured by the implemented VNA are illustrated by figure 5.27. The maximum magnitude error is of -20 dB and the maximum phase error is of 50 degrees.

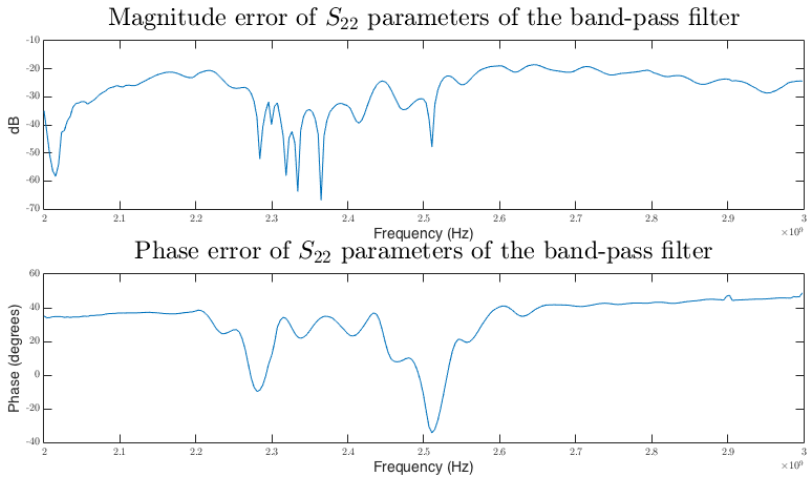

Figure 5.27: Magnitude and phase errors of the S_{22} parameters:
errors between S_{22} parameters measured by the reference VNA and S_{22} parameters measured by the implemented VNA

Figure 5.28 illustrates the S_{21} parameters of the filter measured by the implemented VNA and the S_{21} parameters of the filter measured by the reference VNA.

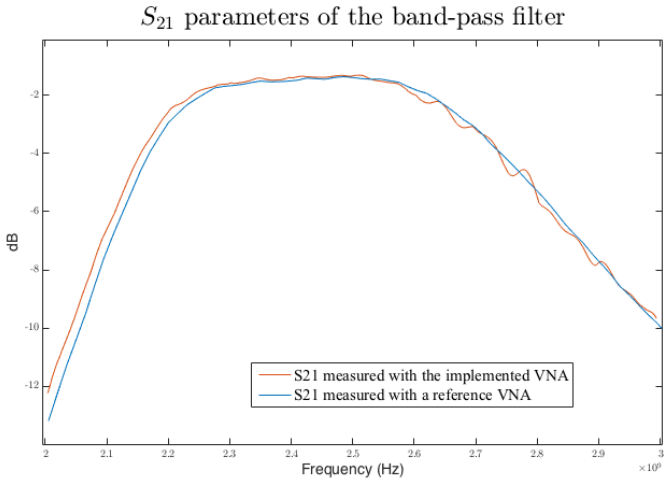

Figure 5.28: S_{21} parameters of the band-pass filter:
measured by the reference VNA vs measured by the implemented VNA

The errors between the S_{21} parameters measured by the reference VNA and the S_{21} parameters measured by the implemented VNA are illustrated by figure 5.29. The maximum magnitude error is of -28 dB and the maximum phase error is of 33 degrees.

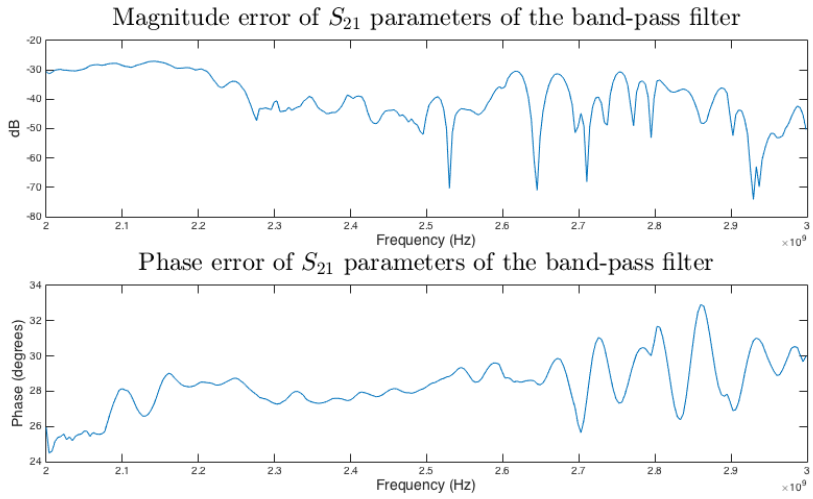

Figure 5.29: Magnitude and phase errors of the S_{21} parameters:
errors between S_{21} parameters measured by the reference VNA and S_{21} parameters measured by the implemented VNA

Figure 5.30 illustrates the S_{12} parameters of the filter measured by the implemented VNA and the S_{12} parameters of the filter measured by the reference VNA.

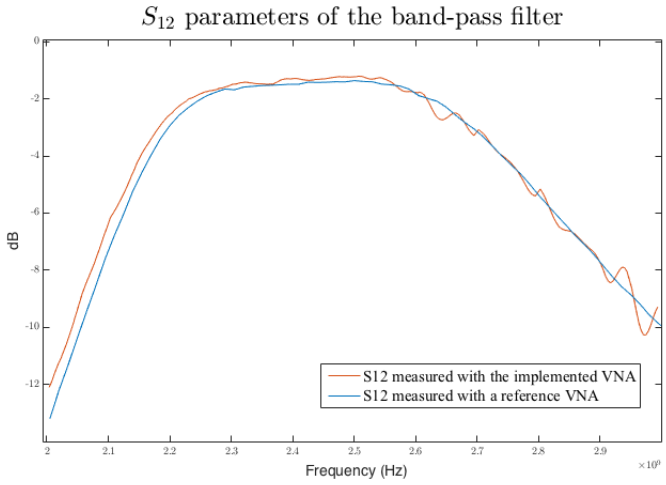

Figure 5.30: S_{12} parameters of the band-pass filter:
measured by the reference VNA vs measured by the implemented VNA

The errors between the S_{12} parameters measured by the reference VNA and the S_{12} parameters measured by the implemented VNA are illustrated by figure 5.25. The maximum magnitude error is of -15 dB and the maximum phase error is of 35.5 degrees.

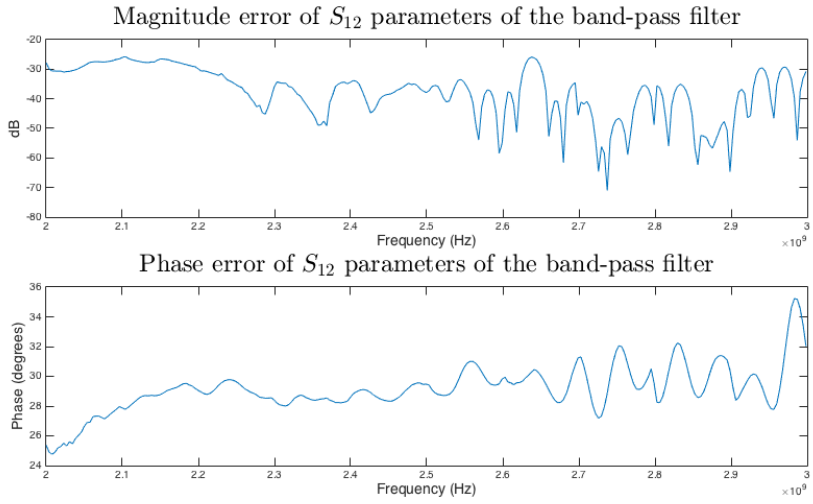

Figure 5.31: Magnitude and phase errors of the S_{12} parameters:
errors between S_{12} parameters measured by the reference VNA and S_{12} parameters measured by the implemented VNA

After analyze the results presented in this subsection is evident that the S-parameters of two-port devices measured by the implemented VNA are affected by a considerable error. The error is more significant on the phase of S-parameters and is probably due to an error on the calibration of the "Thru" standard that was not identified.

Chapter 6

Conclusions

In this dissertation a power meter, an oscilloscope and a VNA were implemented and tested.

The power meter was tested for the entire power range and for three different frequencies covering this way the range from 40 MHz to 3 GHz. The power values obtained are as precise as expected, since the power detector specifies one dB of linearity within the power and frequencies ranges and the maximum error of the measurements made by the power meter is of 1.1 dB.

The proposed oscilloscope was implemented successfully. Some of the systems that are usually implemented on hardware, as the trigger system, were implemented in software (MATLAB®) due to limitations on the hardware used. The communication protocol used between the FPGA and MATLAB® (UART) compromised the waveform update rate of the oscilloscope, even with the maximum baudrate the waveform update rate is low compared with the commercial oscilloscopes. A graphical user interface was built on MATLAB® that allows the user to control the oscilloscope and to visualize the acquired waveforms.

The waveforms of a two tone signal, acquired by the implemented oscilloscope and by a reference sampling oscilloscope were compared. It was verified that the waveform acquired by the implemented oscilloscope corresponds to the envelope of the signal acquired by the reference sampling oscilloscope, as expected.

The VNA was also achieved. The working frequency is limited only by the isolators and directional couplers and VSG used, the rest of the system is designed to work from 300 MHz to 6 GHz. Another important limitation is the fact that the RF receivers have to be switched manually because the RF transceiver only allows to measure synchronously from two RF receivers. For controlling the VNA and visualize the resulting S-parameters, a graphical user interface was created on MATLAB®. For one-port measurements the

VNA presents low error comparing with a reference VNA. For two-port measurements the S-parameters present considerable phase error whose source is unknown at the time of concluding this work.

6.1 Future Work

The implemented oscilloscope uses MATLAB® to process and display the acquired waveforms through a graphical user interface. Instead of using MATLAB®, the oscilloscope could be implemented using only the FPGA and displaying the data in a monitor connected directly to the FPGA. This way the systems implemented on MATLAB® would have higher flexibility, and the bottleneck caused by the data transfer by UART would disappear.

The implemented VNA main limitations are the working frequency, the manual switch of the receivers, and the measuring time. The working frequency can be easily increased by replacing the isolators, the directional couplers and the VSG. The manual switch of the receivers can be replaced by a RF switch controlled by the FPGA, this change would decrease the time for calibrate the VNA and for measure two-port devices. Similarly to the oscilloscope, the measuring time is highly increased by the time for transferring the data between the FPGA and MATLAB®. The data transfer can be speeded up by implementing the Fast Fourrier Transform (FFT) on hardware and send to MATLAB® only the relevant spectral information.

Beyond implementing the FFT on hardware, the entire system could be implemented on FPGA using only a monitor for the user interface. This implementation would allow a deeper control of the hardware and a better performance.

To obtain a more complete RF laboratory it could be also developed a NVNA. To develop a NVNA it could be used the FPGA used for all instruments implemented. The RF transceiver used for on the VNA and oscilloscope would not be enough because a one-port NVNA requires three RF receivers synchronous and a two-port NVNA requires five RF receivers synchronous. The NVNA requires one more RF receiver comparing with the VNA to calibrate the harmonic's phase. To calibrate the harmonic's phase, it can be used a comb generator. To get the necessary RF receivers either can be used a different RF transceiver with the necessary RF receivers or it can be used another AD9371 simultaneously.

Bibliography

[1] Ribeiro D. , "Sistema de Medida Analógico-Digital para Software-Defined Radios", M.S. thesis, DETI, UA, Aveiro, 20111

[2] W. Van Moer and L. Gommé, "NVNA Versus LSNA: Enemies or Friends?", IEEE microwave, Feb 2010

[3] *Principles of Power Measurement: A Primer on RF & Microwave Power Measurement*, Boonton, United States, 2011

[4] A. Fanton, "Bolometers", in *Radio frequency & microwave power measurement*, London, United Kingdom: Peter Peregrinus Ltd, 1990, ch. 6, 72-95

[5] *Practical Radio Frequency Test and Measurement: A Technician's Handbook*, 2002

[6] D.F. Williams, P.D. Hale and Kate A. Remley, "The sampling Oscilloscope as a Microwave Instrument", IEEE microwave, Aug 2007

[7] J. Bird, "Electrical measuring instruments and measurements", in *Electrical and Electronic Principles and Technology*, 5^{th} ed. New York: Routledge, 2014, ch. 10, 119-143

[8] *What is the difference between an equivalent time sampling oscilloscope and a real-time oscilloscope?*, Keysight Tecnologies, USA, 2014

[9] *IEEE Standard for Digitizing Waveform Recorders*, IEEE standard 1057, 2007

[10] *Understanding Key High-Performance Oscilloscope Specifications*, Tektronix, U.S., 2002

[11] N. B. Carvalho and D. Schreurs, "Instrumentation for wireless systems", in *Microwave and Wireless Measurement Techniques* , New York: Cambridge University Press, 2013 , ch. 2, 63-121

[12] N. Shoaib, "General Introduction", in *Vector Network Analyser (VNA) Measurements and Uncertainty Assessment*, Torino, Italy: Springer, ch.1, 1-19

[13] *ZC706 Evaluation Board for the Zynq-7000 XC7Z045 All Programmable SoC User Guide*, Xilinx, 2016,

[14] *System Development User Guide for the AD9371 Integrated, Dual RF Transceiver with Observation Path*, Analog Devices, 2016-2017

[15] Minicircuits ZGBDC20-33HP+ [Online], Available: https://ww2.minicircuits.com/pdfs/ZGBDC20-33HP+.pdf

[16] Narda Isolators, model 4913 [Online], Available: https://nardamiteq.com/docs/113-ISOLATORS.PDF

[17] Linear Technology, DEMO CIRCUIT 1599A [Online], Available: http://cds.linear.com/docs/en/demo-board-manual/dc1599A.pdf

[18] RHODE&SCHWARZ, R&S®SMU200A Vector Signal Generator [Online], Available: https://www.rohde-schwarz.com/us/product/

[19] *Specifying Calibration Standards and Kits for Keysight Vector Network Analyzers*, Keysight Tecnologies, 2016

[20] *Electronic vs. Mechanical Calibration Kits:Calibration Methods and Accuracy*, Keysight Tecnologies, 2014

[21] XAHonnor Scient-tech co., Ltd, SMA Connectors, [Online], Available: http://www.honorconnector.com/sma-connectors/sma-pcb-mount-connectors.html